XX

Photoinduced Reactions of Radical Ions via Charge Separation
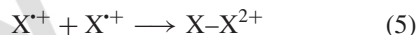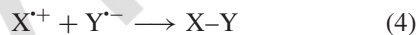
Shunichi Fukuzumi and Kei Ohkubo

Department of Material and Life Science, Graduate School of Engineering, Osaka University, ALCA, Japan Science Technology Agency (JST), Suita, Osaka, Japan and Department of Bioinspired Science, Ewha Womans University, Seoul, Korea

1 INTRODUCTION

Free radicals are highly versatile and reactive intermediates, allowing many synthesis to be carried out under relatively mild conditions in chemical and biological systems (1).[1–5] However, the high reactivity of free radicals usually results in low selectivity (2) and (3). Thus, it has been difficult to utilize reactions between free radicals for selective bond formation[1–5]:

$$X^{\bullet} + Y^{\bullet} \longrightarrow X–Y \qquad (1)$$

$$X^{\bullet} + X^{\bullet} \longrightarrow X–X \qquad (2)$$

$$Y^{\bullet} + Y^{\bullet} \longrightarrow Y–Y \qquad (3)$$

In contrast to neutral free radicals, reactions of radical ions are well controlled by charges: radical cations are expected to react selectively with radical anions (4) as compared with reactions of radical ions with the same charge (5) and (6):

$$X^{\bullet+} + Y^{\bullet-} \longrightarrow X–Y \qquad (4)$$

$$X^{\bullet+} + X^{\bullet+} \longrightarrow X–X^{2+} \qquad (5)$$

$$Y^{\bullet-} + Y^{\bullet-} \longrightarrow Y–Y^{2-} \qquad (6)$$

Thus, reactions between radical cations and radical anions have profound fundamental and synthetic interest for selective bond formation.[6–13] Radical cations and radical anions are formed using electron donor–acceptor-linked molecules, because the photoexcitation results in the formation of the radical ion pair, which can oxidize and reduce substrates to generate the corresponding radical cations and radical anions, respectively.[14–17] Radial cations ($X^{\bullet+}$) and radical anions ($Y^{\bullet-}$) thus produced may couple selectively to produce the coupling products (X–Y) (4) in competition with back electron transfer from $Y^{\bullet-}$ to $X^{\bullet+}$.

Extensive studies have so far been devoted to mimic the function of the photosynthetic reaction center by developing electron donor–acceptor-linked molecules, which undergo a cascade of electron-transfer steps leading to long-range charge separation with prolonged lifetime of the charge-separated (CS) state.[18–40] In a view of synthetic feasibility and their applications, it is important to develop electron donor–acceptor dyads in which the CS states have long lifetimes without losing energy by multistep electron-transfer processes.

This article focuses on reactions of radical ions produced by electron-transfer reactions of the CS state of electron donor–acceptor dyads (D–A) as shown in Scheme 1. First an electron donor–acceptor dyad capable of efficient photoinduced electron transfer to produce a long-lived CS
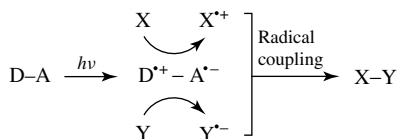
Scheme 1 Radical coupling reaction of $X^{\bullet+}$ and $Y^{\bullet-}$ produced by electron-transfer reactions of substrates (X and Y) with the CS state of an electron donor–acceptor dyad (D–A).

Figure 1 Chemical structure and crystal structure of Acr^+–Mes.[44]

state $(D^{\bullet+}–A^{\bullet-})$ is described. Then, the long-lived CS state is utilized for generation of radical cations $(X^{\bullet+})$ and radical anions $(Y^{\bullet-})$, which are coupled to afford the coupling products (X–Y) (Scheme 1). Radical cations can also be converted to the corresponding neutral radicals by deprotonation, whereas radical anions can be converted to the corresponding neutral radicals by protonation. Thus, combination of deprotonation of radical cations and protonation of radical anions leads to facile reactions of neutral radicals. The reactions of radical cations, which are produced by electron-transfer reactions of the CS state of an electron donor–acceptor dyad, with nucleophiles are also described in this article.

2   FORMATION OF LONG-LIVED CHARGE-SEPARATED STATES

In order to produce radical ions by electron-transfer reactions with a CS state, the CS lifetime must be long enough to compete with back electron transfer to the ground state. The lifetime of the CS state has been reported to be elongated by decreasing the distance between the donor and acceptor in the dyads, which results in a decrease in the solvent reorganization energy of electron transfer.[41] Among many electron donor–acceptor-linked molecules, an acridinium ion is the best candidate as a chromophore as well as an electron acceptor, because of the efficient electron self-exchange between the acridinium ion and the corresponding one-electron reduced radical[7,42] and the high triplet excited energy.[43] Thus, an electron donor moiety (mesityl group) is directly connected at the 9-position of the acridinium ion to yield 9-mesityl-10-methylacridinium ion (Acr$^+$–Mes, Figure 1),[44] in which the solvent reorganization of electron transfer is minimized, because the overall charge remains the same in the charge-shift electron transfer with the short
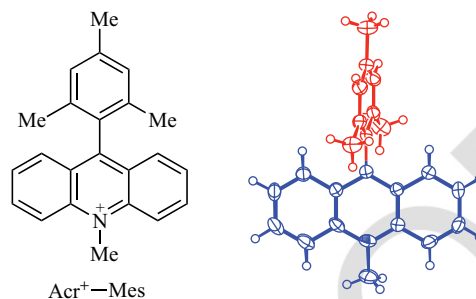
linkage between the donor and acceptor moieties. Acr$^+$–Mes affords the electron-transfer state on photoexcitation with not only a much longer lifetime (e.g., 2 h at 203 K) and a high quantum yield close to unity (98%) but also a much higher energy (2.37 eV) than the natural system.[44]

The rate of intramolecular electron transfer from the $Acr^{\bullet}$ moiety to the $Mes^{\bullet+}$ moiety in the same $Acr^{\bullet}$–$Mes^{\bullet+}$ molecule is highly temperature dependent and the lifetime of the electron-transfer state becomes almost infinite (10^{29} years extrapolated from the Arrhenius plot for BET rates) at 77 K in solid state.[44] Nuclear tunneling usually becomes more apparent at lower temperatures, but this seems not to be the case for $Acr^{\bullet}$–$Mes^{\bullet+}$. The X-ray crystal structure of Acr$^+$–Mes in Figure 1 exhibits that the dihedral angle is perpendicular between the Mes and Acr$^+$ moieties of Acr$^+$–Mes.[44] In such a case, the orbital interaction between the donor and acceptor moieties is minimized. This is the key point to attain the long lifetime of the electron-transfer state. The simple molecular dyad (Acr$^+$–Mes) capable of fast photoinduced electron transfer but relatively slow back electron transfer to the ground state has clear advantages with regard to synthetic feasibility and its application as an organic photocatalyst.[45]

The electron-transfer state of Acr$^+$–Mes has both strong oxidizing and reducing ability that would never be attained by the excited state of the electron acceptor moiety.[44,46] However, there have been some reports on possible formation of the triplet excited state of the acridinium ion moiety rather than the electron-transfer state (Scheme 2).[47–51] It was reported that the photoexcitation of 9-(1-naphthyl)-10-methylacridinium ion (Acr$^+$–1 NA) resulted in the formation of the
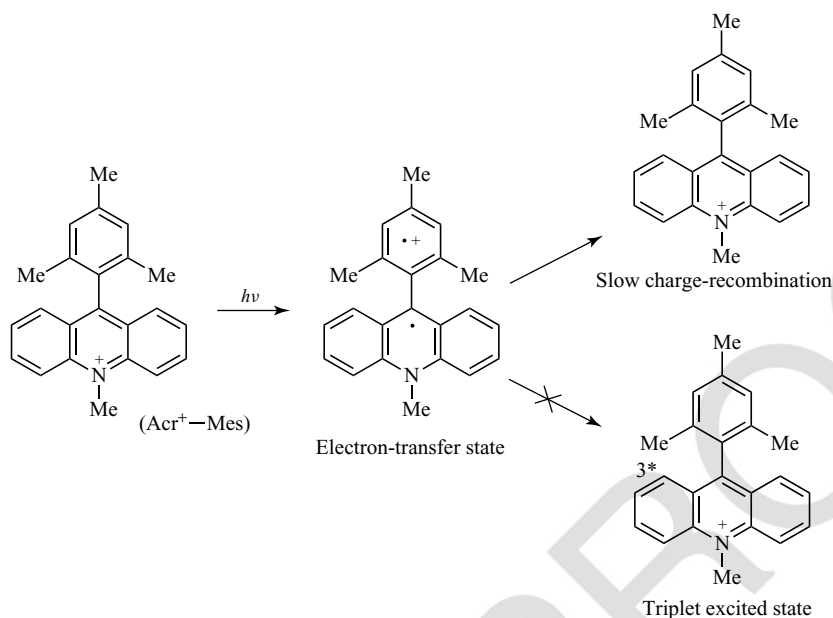
Scheme 2 Reaction course of Acr$^+$–Mes on photoexcitation.
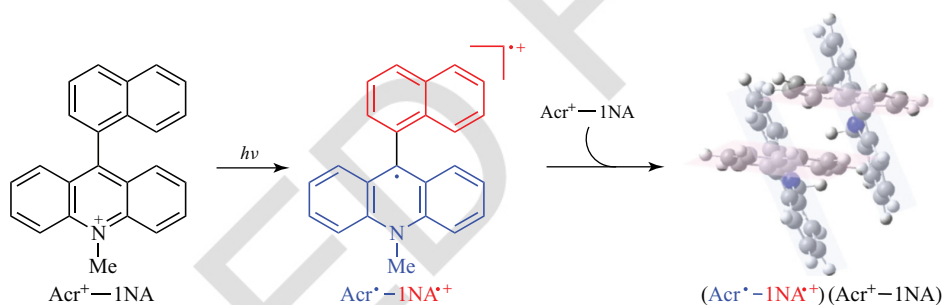
Scheme 3 π-Dimer formation of the electron-transfer state of Acr$^+$–1 NA with the ground state of Acr$^+$–1 NA.

triplet excited state, because of the absence of the transient absorption due to the radical cation at 700 nm.[52–54] The reason why the electron-transfer state of Acr$^+$–1 NA was overlooked was later shown by clear cut evidence of the formation of the electron-transfer state (NOT the triplet excited state) of Acr$^+$–1 NA, which forms the π-dimer radical cation complex with the ground state of Acr$^+$–1 NA (Scheme 3).[55] The nanosecond laser excitation of a deaerated acetonitrile (MeCN) solution of Acr$^+$–1 NA at 355 nm resulted in the appearance of the new absorption band at 1050 nm due to the naphthalene π-dimer radical cation as shown in Figure 2a.[55] The equilibrium between monomer naphthalene radical cation and dimer naphthalene

radical cation is observed in intermolecular photoinduced electron transfer from naphthalene to the singlet excited state of 10-methylacridinium ion (^{1}AcrH$^+$*) as shown in Figure 2b.[55] When the concentration of naphthalene is 10 mM, the transient absorption due to monomer radical cation of naphthalene is clearly seen at 700 nm together with the near-infrared (NIR) absorption at 1050 nm due to the dimer naphthalene radical cation (Figure 2b). When the concentration of naphthalene is increased to 100 mM, the transient absorption at 700 nm due to monomer radical cation of naphthalene disappears, accompanied by an increase in the absorbance at 550 and 1050 nm due to the naphthalene π-dimer radical cation (Figure 2b). The
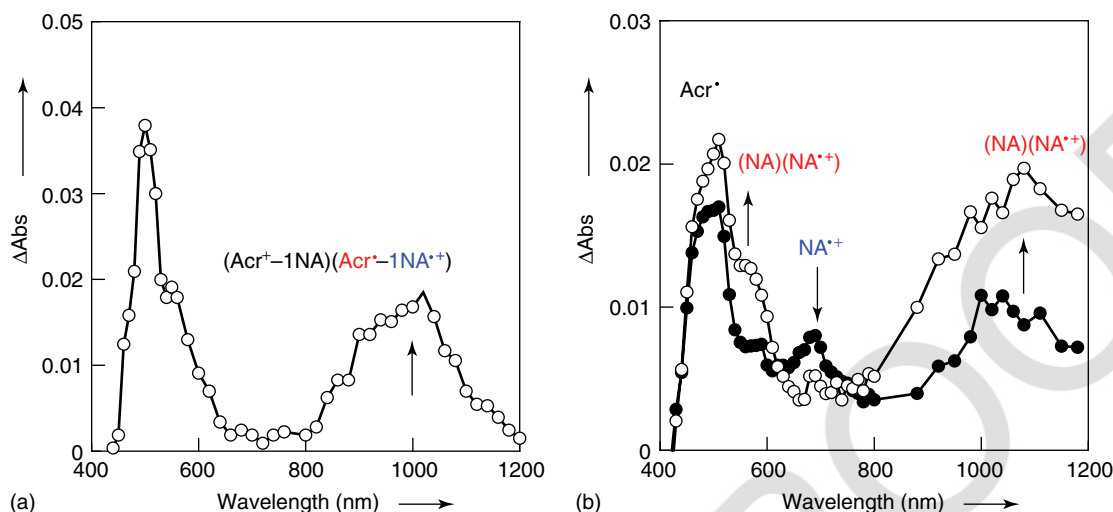
Figure 2 Transient absorption spectra of (a) Acr$^+$–1 NA (5.0×10^{-5} M) and (b) AcrH$^+$ (3.0×10^{-5} M) with 10 mM (•) and 100 mM (◦) of naphthalene in deaerated MeCN at 298 K taken at 2 µs after laser excitation at 355 nm.[55]

broad absorption band in the NIR region due to the π-dimer radical cation was also clearly observed in the case of Acr$^+$–Mes.[55] This is different from the band at 960 nm due to the T–T absorption of 9-phenylacridine.[46,56–58] The formation of stable π-dimer radical cations and anions of aromatic compounds has been well known as a result of π-bonding of neutral π-compounds with the radical cations and radical anions, respectively.[59–66]

The light-havesting capability of Acr$^+$–Mes is significanlty improved by assembling Acr$^+$–Mes molecules on Au nanoclusters (Mes–Acr$^+$–PhS–AuC) as shown in Scheme 4.[67]

The Mes–Acr$^+$–PhS–AuC nanocluster was prepared by the coupling between the functional molecules and Au nanoclusters. Carboxyl-terminated Mes–Acr$^+$–COOH[67,68] is directly coupled to 4-mercaptophenol-functionalized Au nanoclusters (PhS–AuC) in the presence of N,N'-diisopropylcarbodiimide and 4-(N,N-dimethylamino)pyridinium-4-toluene-sulfonate as the standard coupling agents (Scheme 4).[67] The reference compound (Mes–Acr$^+$–COOPh) was synthsized by condensation of Mes–Acr$^+$–COOH and phenol.[67]

Femtosecond laser excitation of Mes–Acr$^+$–PhS–AuC at 420 nm results in appearance of a transient absorption band at 490 nm and a broad transient absorption band in the NIR region as shown in Figure 3a.[67] Such a broad NIR band is assigned to the π-dimer radical

cation of the electron-transfer state of Mes–Acr$^+$ (Mes$^{•+}$–Acr$^•$–PhS–AuC) with the neighboring Mes–Acr$^+$ molecule. This is made possbile by the close proximity of Mes–Acr$^+$ molecules on AuC via an intramolecular π–π interaction on photoinduced electron transfer from the Mes moiety to the singlet excited state of the Acr$^+$ moiety. In contrast to this, no transient absorption band in the NIR region was observed in the case of the reference compound (Mes–Acr$^+$–COOPh), when only the transient absorption band at 490 nm due to the electron-transfer state of Mes–Acr$^+$–COOPh (Mes$^{•+}$–Acr$^•$–COOPh) is observed at 10 ps (Figure 3b).[67] The π-dimer radical cation of Mes$^{•+}$–Acr$^•$–COOPh with Mes–Acr$^+$–COOPh was formed by the intermolecular reaction at 10 µs, in sharp contrast to intramolecular formation of the π-dimer radical cation at 1 ps as shown in Figure 3a.[67] Thus, the photoexcitation of gold nanoclusters (AuC) functionalized with Mes–Acr$^+$ resulted in rapid formation of the electron-transfer state (Mes$^{•+}$–Acr$^•$) to produce the π-dimer radical cation with the neighboring Mes–Acr$^+$ molecule on AuC, whereas such π-dimer radical cation formation occurs at much slower timescale for the reference compound (Mes–Acr$^+$–COOPh) by the intermolecular reaction between Mes$^{•+}$–Acr$^•$–COOPh and Mes–Acr$^+$–COOPh.
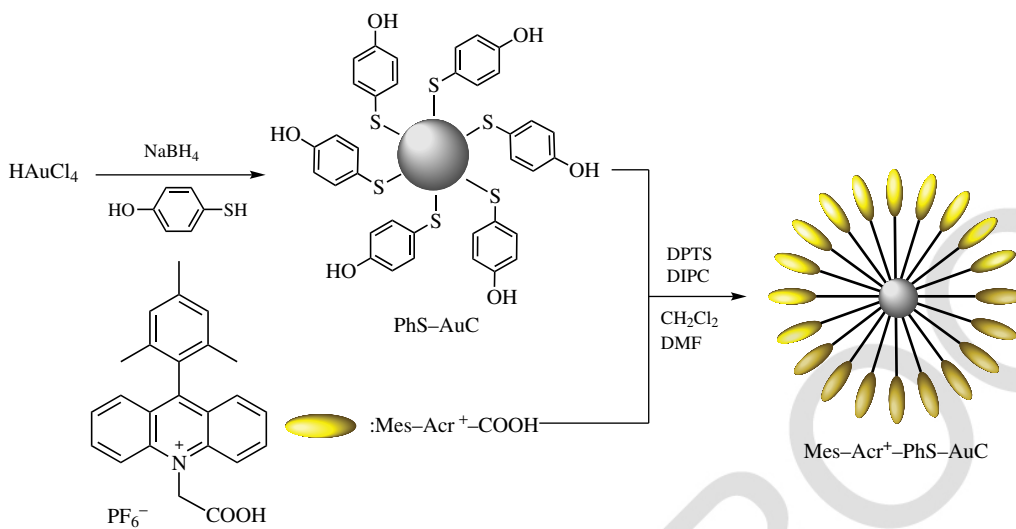
Scheme 4   Preparation of 9-mesitylacridinium ion-monolayer-protected gold nanoclusters (Mes–Acr$^+$–PhS–AuC).[67]
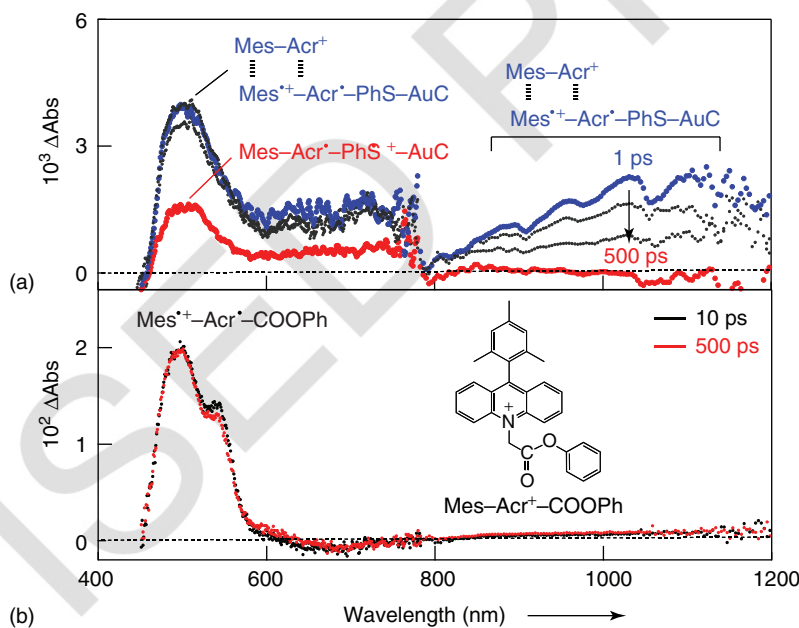

Figure 3   Transient absorption spectra observed in femtosecond laser flash photolysis ($\lambda_{ex} = 420$ nm) of (a) Mes–Acr$^+$–PhS–AuC at 2 and 500 ps and (b) Mes–Acr$^+$–COOPh at 10 and 500 ps in MeCN at 298 K.[67]

Immobilization of Acr$^+$–Mes molecules in a solid porous framework provides a wide range of potential applications, including as solid-state photocatalysts and in electrical devices. Periodic mesoporous organosilicas (PMOs) prepared

by surfactant-directed self-assembly of bridged organosilane precursors ((R′O)$_3$Si–R–Si(OR′)$_3$, R: organic bridging group) have been used to immobilize Acr$^+$–Mes (Scheme 5).[69] PMOs with a high surface area are promising candidates as
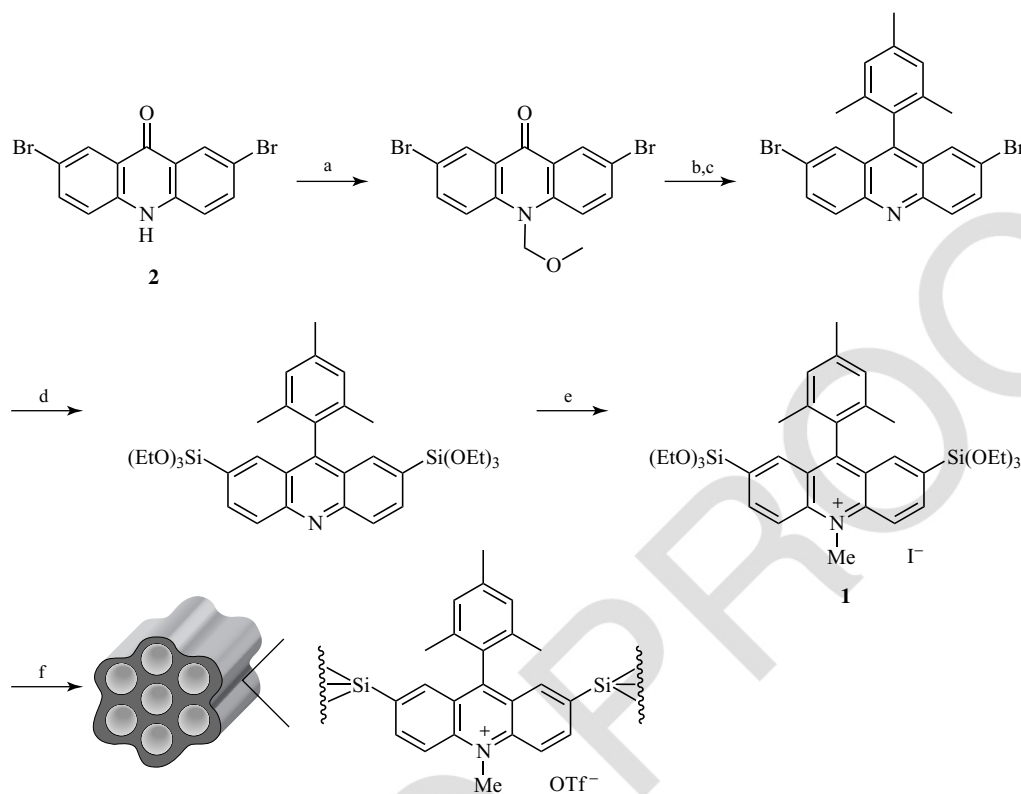
Scheme 5 Synthetic route for the preparation of Mes–Acr$^+$ organosilane precursor **1** and mesostructured organosilica. (a) NaH, MOMCl, dimethylformamide (DMF); (b) MesMgBr, tetrahydrofuran; (c) HCl aq; (d) HSi(OEt)$_3$, NEt$_3$, n-Bu$_4$NI, [Rh(cod)(CH$_3$CN)$_2$]BF$_4$, DMF; (e) MeOTf, CH$_2$Cl$_2$ (X = OTf); (f) Brij76, HCl aq, EtOH.[69]

solid-state functional materials, because their function and morphology can be readily controled by appropriate selection of organic bridges (–R–) within the framework.[70–77] The mesostructured materials were successfully obtained from the newly designed precursor **1** (Scheme 5) without dilution of the scaffold silica sources (e.g., tetraethoxysilane).[69] The Acr$^+$–Mes-bridged precursor **1** was prepared starting from commercially available 2,7-dibromoacridone **2** in 74% overall yield (five steps) (Scheme 5). Photoinduced electron transfer within the Acr$^+$–Mes–silica hybrid framework was demonstrated to afford the electron-transfer state over a microsecond timescale.[69]

The following sections describe the development photocatalytic oxidation, cycloaddition, and bromination via the long-lived electron-transfer state of Acr$^+$–Mes.

## 3 PHOTOOXYGENATION VIA ELECTRON TRANSFER

3.1 Photooxygenation of Anthracene via Radical Ion Coupling

As described above, photoexcitation of Acr$^+$–Mes results in the formation of the electron-transfer state (Acr$^•$–Mes$^{•+}$), which has an extremely long lifetime (e.g., 2 h at 203 K) as well as both highly oxidizing and reducing ability.[44,78] In such a case, Acr$^+$–Mes acts as an efficient electron-transfer photocatalyst for highly selective oxygenation of various substrates with O$_2$ via selective radical ion coupling of the donor radical cation and superoxide anion (O$_2^{•-}$) under visible light irradiation (vide infra).

Visible light irradiation ($\lambda > 430$ nm) of the absorption band of Acr$^+$–Mes in an O$_2$-saturated

MeCN solution containing 9,10-dimethylanthracene (Me_2An) results in the formation of oxygenation product, that is, dimethylepidioxyanthracene ($Me_2An\text{-}O_2$) via efficient [4 + 2] coupling between the radical cation of 9,10-dimethylanthracene ($Me_2An^{•+}$) and $O_2^{•-}$, which are produced by the electron-transfer oxidation of Me_2An and the electron-transfer reduction of O_2 with the electron-transfer state of Acr^+–Mes, respectively, as shown in Scheme 6.[78] Anthracene and 9-methylanthracene also undergo the photocatalytic oxygenation by O_2 with Acr^+–Mes to afford the corresponding epidioxyanthracenes ($An\text{-}O_2$ and $MeAn\text{-}O_2$, respectively) under visible light irradiation.[78] Epidioxyanthracenes are known to be formed by the reaction of anthracenes with singlet oxygen ($^1O_2$).[79] However, the rate constant of the reaction of $^1O_2$ with Me_2An (2.4×10^5 M^{-1} s^{-1}) is much smaller than the rate constant of the radial coupling reaction of $Me_2An^{•+}$ and $O_2^{•-}$ (1.7×10^{10} M^{-1} s^{-1}) in MeCN at 298 K.[78] It was confirmed that no singlet oxygen emission was observed during the photocatalytic oxygenation of Me_2An in an O_2-saturated CD_3CN.[78] Thus, $Me_2An\text{-}O_2$ is formed exclusively by the radical ion coupling between $Me_2An^{•+}$ and $O_2^{•-}$ rather than the reaction of Me_2An and $^1O_2$ as shown in Scheme 6.

In the case of anthracene, further photoirradiation results in the formation of anthraquinone as the final six-electron oxidation product via 10-hydroxyanthrone, accompanied by generation of H_2O_2 as shown in Scheme 7.[78] The photocatalytic oxygenation of anthracenes is initiated by photoexcitation of Acr^+–Mes, which results in the formation of the electron-transfer state ($Acr^•$–Mes$^{•+}$), followed by electron transfer from anthracenes to the Mes$^{•+}$ moiety together with electron transfer from the $Acr^•$ moiety to O_2.[44,78] The resulting anthracene radical cation undergoes radical coupling reactions with $O_2^{•-}$ to produce the epidioxyanthracene ($An\text{-}O_2$).[44,78] The mechanism of the photocatalytic conversion of $An\text{-}O_2$ to 10-hydroxyanthrone is shown in Scheme 7.[78] The electron transfer from $An\text{-}O_2$ to the Mes$^{•+}$ moiety of $Acr^•$–Mes$^{•+}$, produced on photoexcitation of Acr^+–Mes, results in the O–O bond cleavage of $An\text{-}O_2$, followed by facile intramolecular hydrogen transfer to produce 10-hydroxyanthrone radical cation. Then the back electron transfer from $Acr^•$–Mes to 10-hydroxyanthrone radical cation yields 10-hydroxyanthrone to regenerate Acr^+–Mes. 10-Hydroxyanthrone is further oxidized to anthraquinone with $Acr^•$–Mes$^{•+}$, accompanied by reduction of O_2 to yield H_2O_2 (Scheme 7).
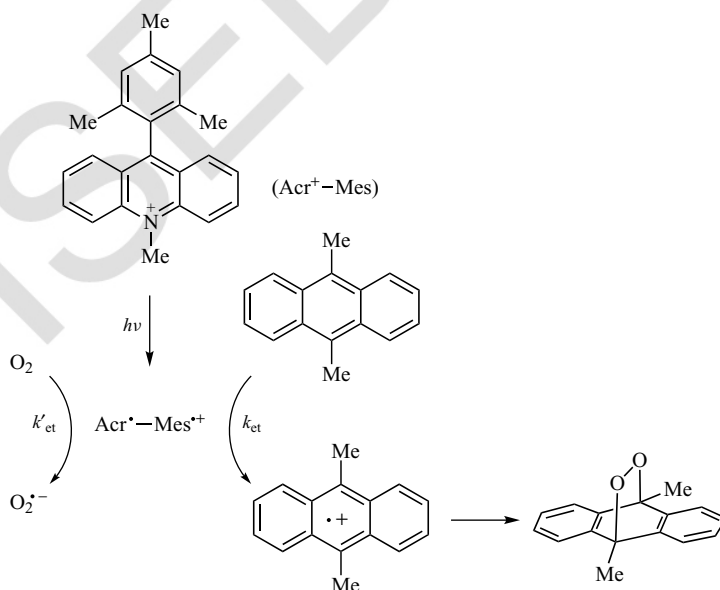
Scheme 6   Photocatalytic oxygenation of Me_2An by O_2 with Acr^+–Mes.[78]
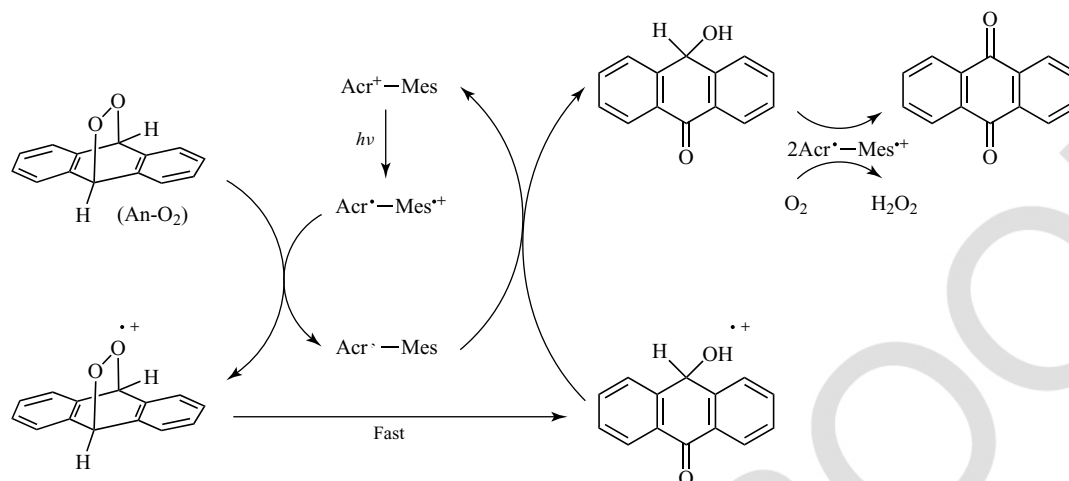
Scheme 7 Photocatalytic oxygenation of anthracene by O_2 with Acr^+–Mes.[78]

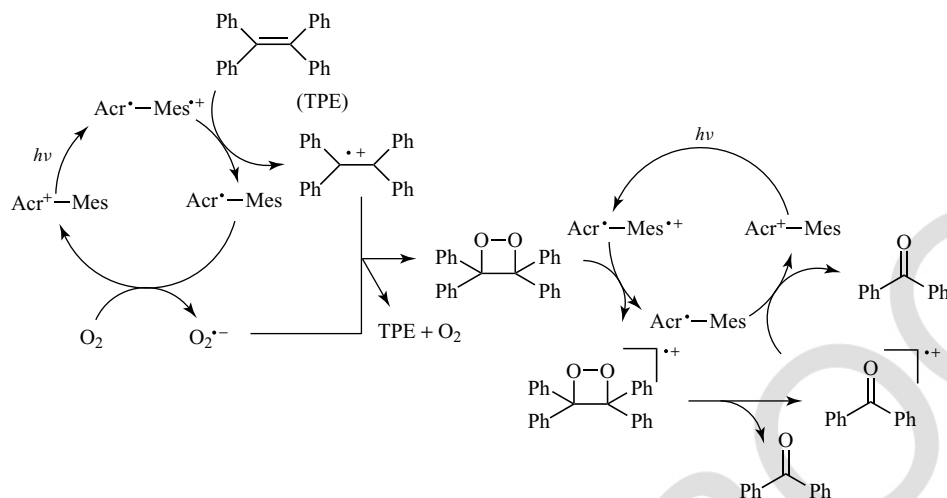## 3.2 Photocatalytic Oxygenation of Tetraphenylethylene to 1,2-Dioxetane

The Acr^+–Mes can also act as an efficient organic photocatalyst for the synthesis of 1,2-dioxetane of tetraphenylethylene (TPE), which would otherwise be impossible to synthesize.[79] 1,2-Dioxetanes have attracted considerable interest because of the key roles in chemiluminescence and bioluminescence,[80–82] which have a broad range of biological, chemical, and medical applications.[83–86] The most common preparation of 1,2-dioxetanes is through the formal $[2 + 2]$ cycloaddition of singlet oxygen ($^1O_2$) to electron-rich alkenes.[87,88] Diastereoselective formation of dioxetanes has also been achieved by a chiral-auxiliary induced $[2 + 2]$ cycloaddition of $^1O_2$ with a chiral allylic alcohol and enecarbamates.[89–93] If alkenes are too electron-poor to react with $^1O_2$, however, no oxygenated products were obtained. For example, no products were formed in an oxygen-saturated MeCN solution of TPE in the presence of $^1O_2$ sensitizers such as C_{60} or tetraphenylporphyrin under photoirradiation.[47] In contrast, the photocatalytic oxygenation of TPE by O_2 occurs efficiently with Acr^+–Mes via the radical ion coupling between TPE radical cation ($TPE^{•+}$) and $O_2^{•-}$, both of which are produced by electron-transfer reactions of TPE and O_2 with the photogenerated electron-transfer state of Acr^+–Mes ($Acr^•$–$Mes^{•+}$),

leading to successful isolation of the corresponding 1,2-dioxetane.[79]

Electron transfer from TPE to the $Mes^{•+}$ moiety in $Acr^•$–$Mes^{•+}$ is energetically feasible, because the one-electron reduction potential of $Acr^•$–$Mes^{•+}$ in MeCN ($E_{red} = 1.88$ V vs SCE, saturated calomel electrode)[44] is more positive than the one-electron oxidation potential of TPE ($E_{ox} = 1.31$ V vs SCE in $CHCl_3$).[79] The second-order rate constant of electron transfer from TPE to $Acr^•$–$Mes^{•+}$ was determined by laser flash photolysis measurements to be 2.5×10^9 M^{-1} s^{-1} in $CHCl_3$, which is close to be the diffusion-limited value as expected from the exergonic electron transfer.[79] The second-order rate constant of the electron-transfer reduction of O_2 by the $Acr^•$ moiety was also determined to be 3.8×10^8 M^{-1} s^{-1} in $CHCl_3$.[79] The formation of $O_2^{•-}$ was confirmed by electron spin resonance (ESR), which was measured at 123 K immediately after the photoirradiation of a chloroform solution of TPE (1.0×10^{-3} M) and Acr^+–Mes (1.0×10^{-4} M) at 233 K.[79] The observed g values agree with those reported for $O_2^{•-}$ ($g_{||} = 2.1050$ and $g_\perp = 2.0032$).[94,95] The transient absorption band of $TPE^{•+}$ decays second-order kinetics.[79] The second-order rate constant was determined to be 6.0×10^9 M^{-1} s^{-1}, which is close to the diffusion-limited value in $CHCl_3$.[79] The bimolecular process involves both the radical coupling between $TPE^{•+}$ and $O_2^{•-}$ to afford the corresponding dioxetane and the back electron transfer from $O_2^{•-}$

Scheme 8 Photocatalytic oxygenation of TPE by O_2 with Acr^+–Mes.[79]

to $TPE^{\bullet+}$ to regenerate the reactant pair as shown in Scheme 8.

The E_{ox} and E_{red} values of the dioxetane were determined by second-harmonic ac voltammetry as 1.56 V and -0.95 V versus SCE, respectively.[79] The E_{ox} value is less positive than the E_{red} value (1.88 V vs SCE in PhCN)[44] of the $Mes^{\bullet+}$ moiety of $Acr^{\bullet}$–$Mes^{\bullet+}$, whereas the E_{ox} value of the $Acr^{\bullet}$ moiety (-0.57 V vs SCE) is less negative than the E_{red} value of the dioxetane. In such a case, the dioxetane is further oxidized by $Acr^{\bullet}$–$Mes^{\bullet+}$ rather than by being reduced to produce the dioxetane radical cation, which undergoes the O–O bond homolysis to produce benzophenone and the radical cation as shown in Scheme 8.[79] The benzophenone radical cation is reduced by $Acr^{\bullet}$–Mes to produce another benzophenone molecule, accompanied by regeneration of Acr^+–Mes (Scheme 8). The thermal oxygenation reaction of TPE with oxygen has previously been proposed to proceed via radical chain processes as shown in Scheme 9.[96–98] The dioxetane is assumed to be produced by direct oxygenation of the dioxetane radical cation with O_2. However, the saturated dependence of Φ on [TPE] and also on [O_2] indicates that such an electron-transfer radical chain process (Scheme 9) is not operative as the major pathway under the photocatalytic reaction conditions.[79]

The formation of the dioxetane radical cation was confirmed by ESR measurements under photoirradiation at low temperature as shown in Figure 4.[79]
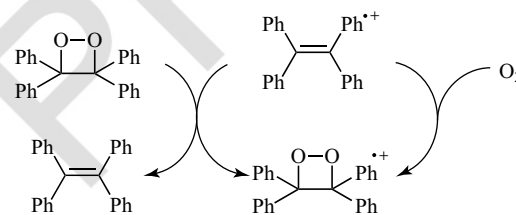
Scheme 9 Radical chain process of photooxygenation of TPE via the dioxetane.

A deaerated chloroform solution of Acr^+–Mes with TPE dioxetane was irradiated by a high-pressure Hg lamp at 223 K. The resulting ESR spectrum observed at 143 K exhibits anisotropic signals at $g_{||} = 2.020$ and $g_\perp = 2.004$. The isotropic g value (g_{iso}) is determined as 2.009 ± 0.001, which agrees with the reported value of a dioxetane radical cation (2.0099).[99] The formation of TPE dioxetane radical cation was also confirmed by photoinduced electron-transfer oxidation of TPE dioxetane with the singlet excited state of 9,10-dicyanoanthracene (DCA) ($^1E_{red}^* = 1.97$ V vs SCE) in frozen deaerated $CHCl_3$ at 143 K.[79] The resulting ESR signal was virtually the same as that shown in Figure 4a.[79] The singly occupied molecular orbital (SOMO) of dioxetane radical cation involves O–O antibonding orbital (Figure 4b).[79] This may be the reason why the facile cleavage of the O–O bond of the dioxetane radical cation occurs to yield benzophenone.[100]
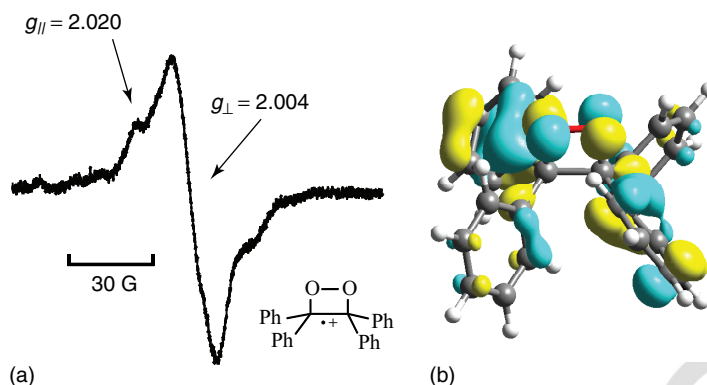
Figure 4 (a) ESR spectrum of TPE dioxetane radical cation observed under irradiation of a deaerated CHCl$_3$ solution containing TPE dioxetane (3.0×10^{-3} M) and Acr$^+$–Mes (3.7×10^{-2} M) at 223 K measured at 143 K (frozen). (b) The SOMO orbital of TPE dioxetane radical cation, calculated by DFT method using UB3LYP/6-31G* basis set.[79]
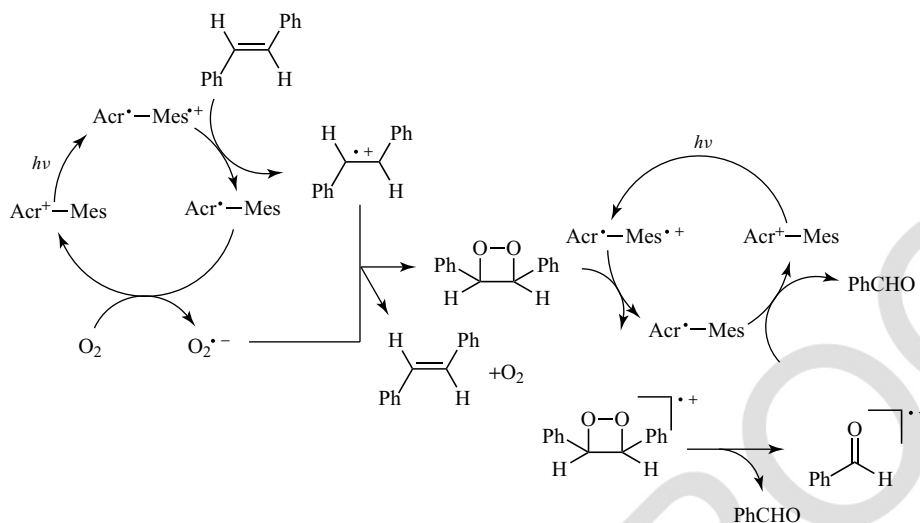
Photocatalytic oxygenation of olefins such as stilbene derivatives also occurs with Acr$^+$–Mes in MeCN and CHCl$_3$.[101] In contrast to the case of TPE, the dioxetane intermediates were not detected under the same experimental conditions as employed for TPE.[101] This indicates that the stilbene dioxetanes decompose to the corresponding benzaldehydes spontaneously under the photoirradiation. The yields of benzaldehyde derivatives obtained from *trans*-stilbene derivatives increase in order: R^1, R^2 = H, H < Me, Me < *p*-MeO, H, as the one-electron oxidation potential (E_{ox}) values of stilbene derivatives decrease.[101] The photooxygenation mechanism of *cis*–stilbene catalyzed by Acr$^+$–Mes is shown in Scheme 10,[101] which is similar to that of TPE (Scheme 8). Electron transfer from stilbene derivatives to the Mes$^{\bullet+}$ moiety of Acr$^\bullet$–Mes$^{\bullet+}$ is energetically feasible, because the E_{ox} values of stilbene derivatives (0.55–1.58 V vs SCE) are less positive than the E_{red} value of the Mes$^{\bullet+}$ moiety of Acr$^\bullet$–Mes$^{\bullet+}$ in PhCN (1.88 V vs SCE).[44] Because stilbene radical cation has low reactivity toward O$_2$,[102–112] the photocatalytic oxygenation of stilbene with Acr$^+$–Mes occurs via the radical ion coupling between stilbene radical cation and O$_2^{\bullet-}$ rather than via the reaction of stilbene radical cation with O$_2$, accompanied by the isomerization of the stilbene radical cation.[101] The stilbene radical cation reacts with O$_2^{\bullet-}$ to produce the dioxetane that decompose spontaneously to benzaldehyde and benzaldehyde radical cation by the electron-transfer oxidation with the Mes$^{\bullet+}$ moiety of Acr$^\bullet$–Mes$^{\bullet+}$. The back electron transfer from Acr$^\bullet$–Mes to benzaldehyde radical

cation yields benzaldehyde to regenerate Acr$^+$–Mes (Scheme 10).

Photocatalytic isomerization of *cis*–stilbene to *trans*-stilbene also occurs with Acr$^+$–Mes in an O$_2$-saturated MeCN as shown in Scheme 10.[101] The concentration of *cis*–stilbene decreases with a concomitant increase due to *trans*-stilbene, when the total concentration of *cis*- and *trans*-stilbene only slightly decreases together with an accompanied increase in the photooxygenation product, benzaldehyde.[101] The observed yield of *trans*-stilbene was 96% after 60-min photoirradiation ($\lambda > 430$ nm), when the total consumption of *cis*- and *trans*-stilbene is still 4%.[101] It is well known that cis-trans isomerization occurs rapidly in the stilbene radical cation.[113–116] The steady-state cis-trans ratio of stilbene has been reproted to be 99:1.[116] Thus, Acr$^+$–Mes acts as a photocatalyst for the cis-trans isomerization of stilbene via the radical cation (Scheme 10).

3.3 Photocatalytic Oxygenation of *p*-Xylene and Reduction of Oxygen

As described above, photocatalytic oxygenation of aromatic substrates occurs via radical ion coupling of the substrate radical cation and O$_2^{\bullet-}$. This section describes photocatalytic oxygenation via the electron-transfer state of Acr$^+$–Mes without radical coupling. Oxygenation of aromatic compounds to produce aromatic aldehydes is key chemical reactions for production of precursors of a variety of
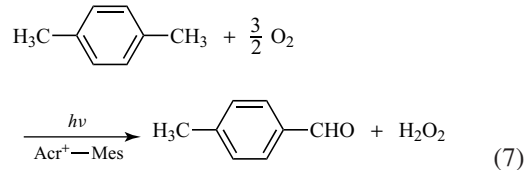
Scheme 10 Photocatalytic isomerization and oxygenation of stilbene by O_2 with Acr^+–Mes.[101]

fine or specialty chemicals such as pharmaceutical drugs, dyestuffs, pesticides, and perfume compositions. A number of methods using inorganic heavy metal oxidants have so far been reported for oxygenation of aromatic compounds to produce the corresponding aldehydes.[117–122] However, their synthetic utility has been limited because of low yield and poor selectivity. Moreover, the use of stoichiometric amounts of inorganic oxidants should be avoided because of the environmental problems.[123] For this reason, catalytic oxygenation processes with molecular oxygen or hydrogen peroxide (H_2O_2) have merited increasing attention.[124] H_2O_2 is in brisk demands for clean and mild oxidant because the byproduct in oxygenation of substrates is only H_2O.[124,125] There have been extensive studies on photocatalytic formation of H_2O_2[126,127] or photocatalytic oxygenation of aromatic substrates.[128–133] If valuable aromatic aldehydes can be produced together with H_2O_2 in the photocatalytic oxygenation of alkyl aromatic compounds by O_2, such a process would be superior as compared to the conventional methods to produce either or both H_2O_2 and aromatic aldehydes.

Such selective photocatalytic oxygenation has been made possible using Acr^+–Mes and its derivative, which act as efficient photocatalysts for simultaneous production of aromatic aldehydes and H_2O_2 in the photocatalytic oxygenation of alkyl aromatic compounds by O_2 under visible light irradiation.[134] Visible light irradiation of $[Acr^+–Mes]ClO_4^-$ ($\lambda_{max} = 430$ nm, 0.20 mM) in oxygen-saturated MeCN containing p-xylene (4.0 mM) with a xenon lamp attached with a color glass filter ($\lambda = 380$–500 nm) for 80 min resulted in formation of an oxygenated product, p-tolualdehyde (34%), p-methylbenzyl alcohol (10%), and H_2O_2 (30%). The overall stoichiometry of the photocatalytic reaction is given by (7).[134] p-Methylbenzyl alcohol is an intermediate in the photocatalytic oxygenation (*vide infra*):

$$H_3C-\!\!\!\bigcirc\!\!\!-CH_3 \; + \; \tfrac{3}{2}\,O_2$$

$$\xrightarrow[\text{Acr}^+-\text{Mes}]{h\nu} \; H_3C-\!\!\!\bigcirc\!\!\!-CHO \; + \; H_2O_2 \tag{7}$$

The photocatalytic reactivity was enhanced by the presence of H_2O (0.9 M) and sulfuric acid (1.0 mM) to yield p-tolualdehyde (75%), p-methylbenzyl alcohol (15%), and H_2O_2 (74%) with a high quantum yield (0.25).[134] The 100% yields of p-tolualdehyde and H_2O_2 with a higher quantum yield (0.37) were achieved using 9-mesityl-2,7,10-trimethylacridinium ion (Me_2Acr^+–Mes), where the hydrogens at 2 and 7 positions of the acridinium ring are replaced by the methyl groups (Table 1).[134]

Table 1　Products and quantum yields for photocatalytic oxygenation of methyl-substituted benzenes with acridinium ion derivatives in O_2-saturated MeCN.[134]

Photocatalyst	Substrate	E_{ox} vs SCE (V)[a]	Yield (%)[b] aldehyde/alcohol/H_2O_2	Quantum yield[b,c]
Acr^+–Mes	p-Xylene	1.93	75/15/74 (34/3/30)	0.25 (0.13)
	Mesitylene	1.71	77/19/75 (47/3/44)	0.30 (0.078)
	Durene	1.63	75/15/70 (35/1/33)	0.30 (0.065)
Me_2Acr^+–Mes	p-Xylene	1.93	100/0/100 (54/5/52)	0.37 (0.13)
	Mesitylene	1.71	66/2/65 (40/1/39)	0.26 (0.14)
	Durene	1.63	64/10/62 (37/2/36)	0.25 (0.15)
Acr^+–Ph	p-Xylene	1.93	12/18/10 (5/2/4)	0.042 (0.019)

[a] Taken from Ref. 42.
[b] Values are determined after photoirradiation for 80 min. Conditions: [photocatalyst] = 0.2 mM, [substrate] = 4.0 mM, [H_2O] = 0.9 M, [H_2SO_4] = 1.0 mM. Values in parentheses are determined without H_2O and H_2SO_4.
[c] On the basis of formation of the corresponding aldehyde.

No further oxygenated product, p-toluic acid or p-phthalaldehyde, was produced during the photocatalytic reaction. When the concentration of Me_2Acr^+–Mes $(1.0 \times 10^{-4}$ M) was decreased, turnover number (TON) was increased to 200. A preparative scale photocatalytic reaction with p-xylene (0.5 g, 4.7 mmol) and Me_2Acr^+–Mes (60 mg, 0.14 mmol) in MeCN (150 ml) under irradiation with a xenon lamp for 48 h afforded p-tolualdehyde (59%), p-methylbenzyl alcohol (28%), and H_2O_2 (51%) with 87% conversion of substrate.[134] The catalyst can be recyclable because no decomposition of photocatalyst occurred under the present experimental conditions.[134] Figure 5 shows the time profiles of the reactant and products in optimized photocatalytic reaction conditions. p-Methylbenzyl alcohol was formed as a reaction intermediate and this was readily oxygenated to form p-methylbenzaldehyde.[134]

The photocatalytic oxygenation also occurred in the case of durene and mesitylene.[134] The one-electron oxidation potentials (E_{ox}) of toluene derivatives in MeCN are listed in Table 1. The E_{ox} values of toluene derivatives given in Table 1 are lower than the one-electron reduction potential (E_{red}) of the electron-transfer state of Acr^+–Mes ($Acr^\bullet$–$Mes^{\bullet+}$: 2.06 V vs SCE in MeCN).[134] Thus, electron transfer from toluene derivatives such as p-xylene to the $Mes^{\bullet+}$ moiety of $Acr^\bullet$–$Mes^{\bullet+}$ is energetically feasible, whereas electron transfer from toluene (E_{ox} = 2.20 V)[42,134] to the $Mes^{\bullet+}$ moiety is energetically unfavorable when no photocatalytic oxidation of toluene by O_2 occurred with Acr^+–Mes under the same experimental conditions.[134]
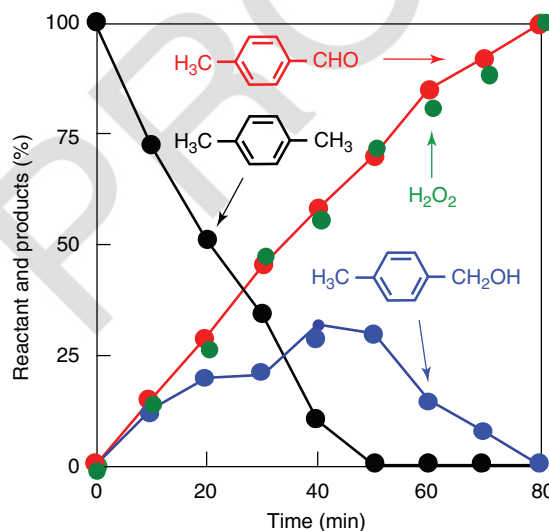

Figure 5　Irradiation time profiles of photooxygenation of p-xylene $(4.0 \times 10^{-3}$ M) catalyzed by Me_2Acr^+–Mes in oxygen-saturated MeCN (0.6 ml) at 298 K; [Me_2Acr^+–Mes] = 2.0×10^{-4} M; [H_2O] = 0.9 M; [H_2SO_4] = 1.0×10^{-3} M.[134]

The E_{ox} values of the oxygenated products of the corresponding benzaldehydes are also higher than the E_{red} value of $Acr^\bullet$–$Mes^{\bullet+}$ (2.06 V).[134] This is the reason why the oxygenated product of p-xylene was only p-tolualdehyde and no further oxygenated product such as p-phthalaldehyde was formed.

The photocatalytic reaction is initiated by intramolecular photoinduced electron transfer from the mesitylene moiety to the singlet excited state of the Acr^+ moiety of Acr^+–Mes, which affords the electron-transfer state ($Acr^\bullet$–$Mes^{\bullet+}$).[44,134] Electron transfer from p-xylene to the $Mes^{\bullet+}$
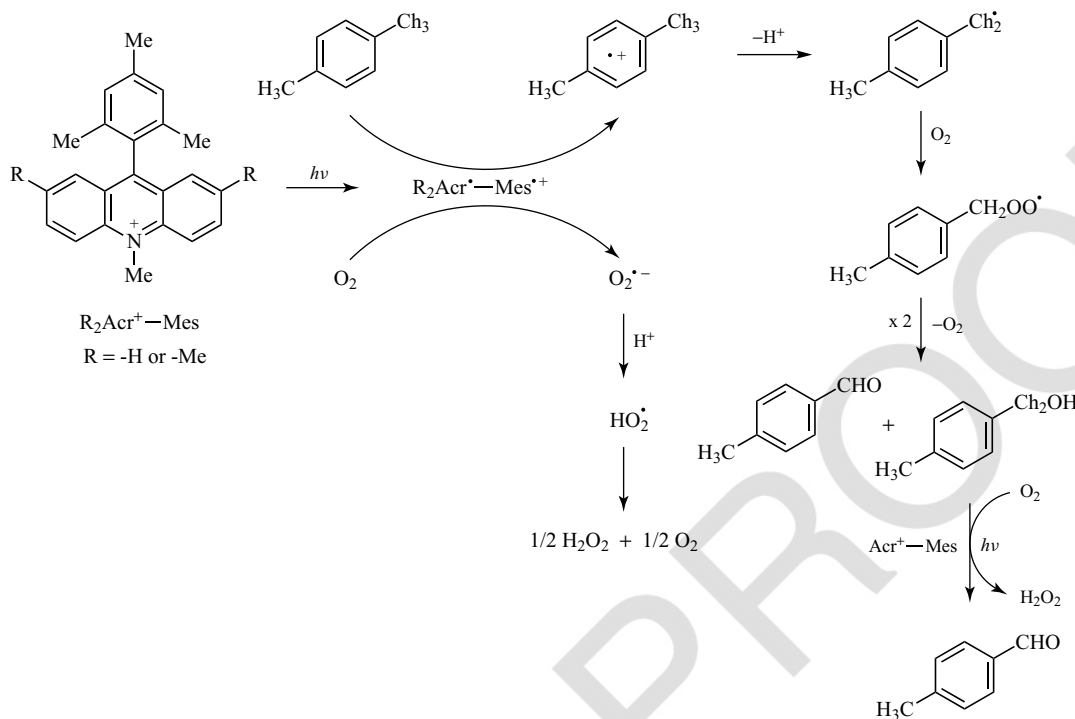
Scheme 11 Photocatalytic oxygenation of p-xylene by O_2 with Acr$^+$–Mes.[134]

moiety occurs to produce p-xylene radical cation, which undergoes deprotonation to afford the deprotonated radical. This is followed by rapid O_2 addition to afford the peroxyl radical as shown in Scheme 11.[134] The disproportionation of the peroxyl radical affords p-tolualdehyde, p-methylbenzyl alcohol, and O_2. p-Methylbenzyl alcohol is readily oxygenated to yield p-tolualdehyde with Acr$^•$–Mes$^{•+}$.[134] On the other hand, $O_2^{•-}$ disproportionates with proton to yield H_2O_2 and O_2 (Scheme 11). The radical intermediates involved in Scheme 11 were detected by ESR ($g_{||} = 2.101, g_\perp = 2.009$ for $O_2^{•-}$ and $g_{||} = 2.033, g_\perp = 2.006$ for p-methylbenzyl peroxyl radical) in frozen MeCN.[134]

Addition of aqueous sulfuric acid enhanced the deprotonation of p-xylene radical cation and the disproportionation process of $O_2^{•-}$, respectively, leading to a remarkable enhancement of photocatalytic reactivity as mentioned above (Table 1).[134] The reaction pathway of photocatalytic oxygenation of p-xylene by O_2 with Acr$^+$–Mes is not the radical chain process, because there was no dependence of the product quantum yield on concentration
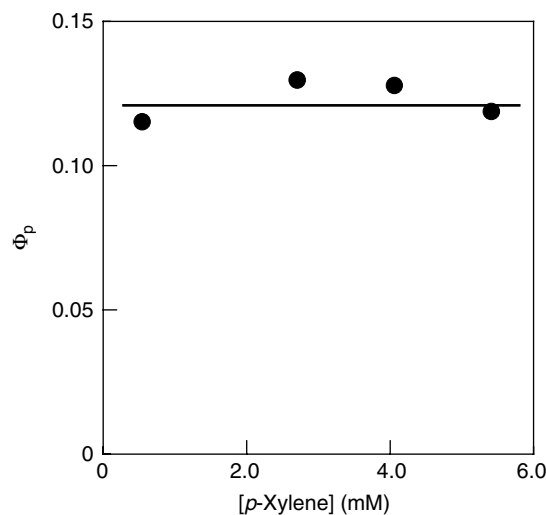
Figure 6 Dependence of quantum yield of formation of p-tolualdehyde on concentration of p-xylene in the photocatalytic oxygenation of p-xylene with Me$_2$Acr$^+$–Mes (0.2 mM) in O_2-saturated MeCN.[134]

of p-xylene (Figure 6) and irradiation light intensity.[134] If the radical chain (autoxidation) process is

involved in the photocatalytic reaction, the quantum yield would increase linearly with increasing concentration of p-xylene, because the rate-determining step in the radical chain process would be the hydrogen abstraction from p-xylene by the peroxyl radical. In addition, there is no induction period that is typically observed for an autoxidation process. Thus, disproportionation of the peroxyl radicals (p-methylbenzyl peroxyl radical and hydrogen peroxyl radical as shown in Scheme 11) is the major pathway in the photocatalytic oxygenation of p-xylene by O_2 with Acr^+–Mes.

In contrast to the case of Acr^+–Mes, the photocatalytic oxygenation of p-xylene by O_2 with Acr^+–Ph that contains no electron donor moiety proceeds via electron transfer from p-xylene to the singlet excited state of Acr^+–Ph. However, the lifetime of the singlet excited state of Acr^+–Ph ($\tau = 1.5$ ns in MeCN)[133] is much shorter than that of the electron-transfer state of Acr^+–Mes. A high concentration of substrate is thereby needed to quench the short-lived singlet excited state of Acr^+–Ph.

2-Methylnaphthalene that does not react with singlet oxygen (i.e., no conversion under irradiation conditions in the presence of tetraphenylporphyrin as a singlet oxygen photosensitizer) is also efficiently oxygenated by O_2 with Acr^+–Mes acting as a photocatalyst to yield the corresponding naphthaldehyde.[135,136] DCA also acts as a photocatalyst for the oxygenation of 2-methylnaphthalene by O_2 as a result of the photoinduced oxidation of 2-methylnaphthalene, followed by deprotonation from the methyl group, and O_2 addition,[135] which is similar to photocatalytic oxygenation of p-xylene by O_2 with Acr^+–Mes as shown in Scheme 11.

The reducing ability of the electron-transfer state of Acr^+–Mes is improved by the electron-donating methyl substitution of the acridinium ring of Acr^+–Mes.[134] Cyclic voltammograms of Acr^+–Mes and Me_2Acr^+–Mes in deaerated MeCN are shown in Figure 7 to compare the reducing abilities of the electron-transfer states of Acr^+–Mes and Me_2Acr^+–Mes.[134] The E_{red} value of Me_2Acr^+–Mes (-0.67 V vs SCE) is 0.1 eV more negative than that of Acr^+–Mes (-0.57 V).[134]

The difference in dynamics of the electron-transfer reduction of O_2 by the electron-transfer states of Acr^+–Mes and Me_2Acr^+–Mes was determined by nanosecond laser flash photolysis.[134] As shown in Figure 8a, the rates of the electron-transfer reduction were determined
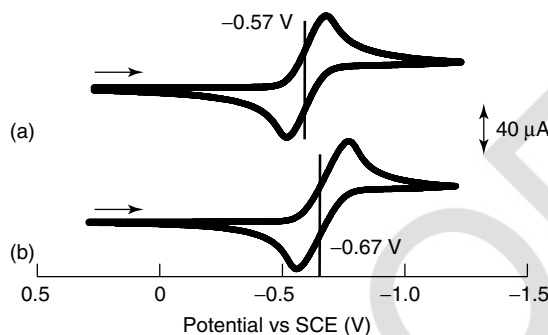

Figure 7 Cyclic voltammograms of (a) Acr^+–Mes and (b) Me_2Acr^+–Mes (10 mM) in deaerated MeCN containing $TBAPF_6$ (0.1 M) at 298 K.[134]

from the quenching of the transient absorption due to the electron-transfer state by O_2 to be 6.8×10^8 M^{-1} s^{-1} for $Acr^•$–$Mes^{•+}$[78] and 2.0×10^{10} M^{-1} s^{-1} for $Me_2Acr^•$–$Mes^{•+}$ (Figure 8b).[134] Thus, the reducing ability of $Me_2Acr^•$–$Mes^{•+}$ was indeed significantly enhanced by the methyl substitution. This may be the reason why the 100% yield of tolualdehyde and H_2O_2 with a higher quantum yield (0.37) was achieved using Me_2Acr^+–Mes (Table 1).

As described above, the electron-transfer state of Me_2Acr^+–Mes, which has both the high oxidizing and reducing ability, make it possible to produce both aromatic aldehydes and H_2O_2 selectively in the photocatalytic oxygenation of alkylaromatic compounds with oxygen. After aromatic aldehydes are formed, no further oxidation takes place because electron transfer from aromatic aldehydes to the $Mes^{+•}$ moiety is thermodynamically unfavorable. Thus, the use of charge-separation dyads as photocatalysts paves a new way for the selective oxygenation of alkylaromatic compounds with simultaneous formation of H_2O_2.

3.4 Photocatalytic Oxygenation of Triphenylphosphine

The photocatalytic oxygenation of triphenylphosphine by O_2 also occurs with Acr^+–Mes.[137]

Visible light irradiation ($\lambda > 430$ nm) of the absorption band of Acr^+–Mes in an O_2-saturated chloroform ($CHCl_3$) solution containing triphenylphosphine (Ph_3P) for 30 min by xenon lamp
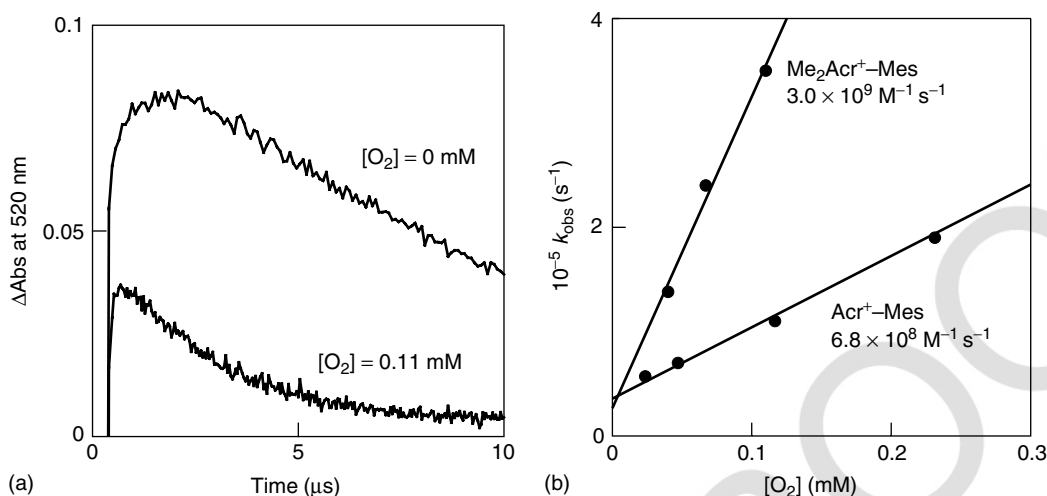
Figure 8 (a) Absorbance time profiles at 520 nm due to $Me_2Acr^\bullet-Mes^{\bullet+}$ in aerated and deaerated MeCN containing Me_2Acr^+-Mes (1.0×10^{-4} M). (b) Plot of the pseudo-first-order rate constant (k_{obs}) for electron transfer from the $Acr^\bullet$ moiety of $Acr^\bullet-Mes^{\bullet+}$ and $Me_2Acr^\bullet-Mes^{\bullet+}$ to O_2 versus $[O_2]$.

results in formation of an oxygenated product, that is, triphenylphosphine oxide ($Ph_3P=O$) with 99% yield[137]:

$$2Ph_3P + O_2 \xrightarrow[Acr^+-Mes]{h\nu} 2Ph_3P=O \qquad (8)$$
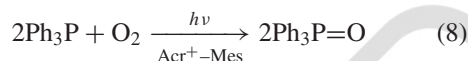
When Acr^+-Mes is replaced by 10-methyl-acridinium ion ($AcrH^+$) with has no electron donor moiety, $Ph_3P=O$ was also produced quantitatively after 60-min photoirradiation.[137] No photooxygenation of Ph_3P occurs without Acr^+-Mes or $AcrH^+$ under otherwise the same experimental conditions.[137] The dependence of the quantum yields (Φ_P) of formation of $Ph_3P=O$ on concentration of Ph_3P is shown in Figure 9 (closed circle).[137] The limiting value (Φ_∞) in air-saturated $CHCl_3$ is constant (0.58) at any Ph_3P concentrations. Judging from the constant dependence of Φ_P on $[Ph_3P]$ in Figure 9 (closed circle), a reactive intermediate of photooxygenation is assigned as an extremely long-lived species, which is the electron-transfer state of Acr^+-Mes.[44] Thus, the rate-determining step in the photocatalytic reaction is proposed to be electron transfer from Ph_3P to $Acr^\bullet-Mes^{\bullet+}$.[137]

In the case of $AcrH^+$ (closed square in Figure 9), the Φ_P values increase on increasing the Ph_3P to higher concentrations than in the case of Acr^+-Mes. From the saturated dependence of Φ_P on $[Ph_3P]$ and the lifetime of $^1AcrH^{+*}$ ($\tau = 31$ ns),[131–133] the
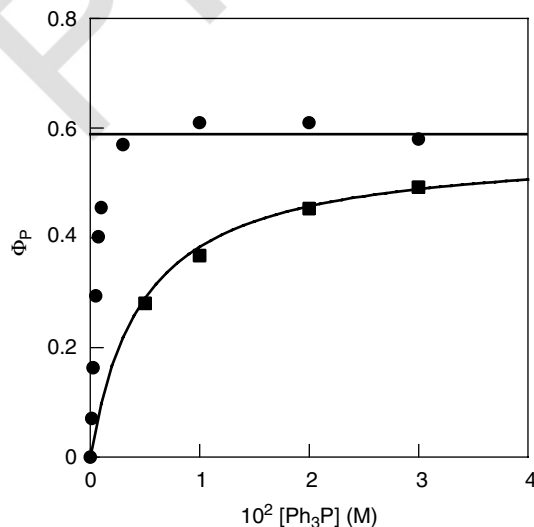

Figure 9 Dependence of quantum yield (Φ_p) on concentrations of Ph_3P for the photocatalytic oxygenation of Ph_3P by O_2 with Acr^+-Mes (8.0×10^{-5} M, $\bullet$) and $AcrH^+$ (8.0×10^{-5} M, $\blacksquare$) in air-saturated $CHCl_3$.

rate constant of the reaction of $^1AcrH^{+*}$ with Ph_3P is 6.8×10^9 M^{-1} s^{-1}, which agrees with the value obtained from the fluorescence quenching of $AcrH^+$ (9.0×10^9 M^{-1} s^{-1}).[137] Such agreement strongly indicates that the photooxygenation of Ph_3P with $AcrH^+$ proceeds via photoinduced electron transfer

from Ph_3P to $^1AcrH^+*$. However, $AcrH^+$-catalyzed photooxygenation requires the high concentrations of Ph_3P and O_2 because the lifetime of $^1AcrH^+*$ is too short to quench the excited state.[137]

Electron transfer from Ph_3P to the $Mes^{\bullet+}$ moiety in $Acr^{\bullet}$–$Mes^{\bullet+}$ is energetically feasible, because the one-electron reduction potential of $Acr^{\bullet}$–$Mes^{\bullet+}$ ($E_{red} = 2.06\,V$ vs SCE)[134] is more positive than the one-electron oxidation potential of Ph_3P ($E_{ox} = 1.20\,V$ vs SCE).[137] The formation of Ph_3P radical cation ($Ph_3P^{\bullet+}$: $\lambda_{max} = 330\,nm$)[137] was confirmed by the laser flash photolysis.[137] The second-order rate constant of electron transfer from Ph_3P to the $Mes^{\bullet+}$ moiety of $Acr^{\bullet}$–$Mes^{\bullet+}$ was determined to be $9.2 \times 10^9\ M^{-1}\ s^{-1}$,[137] which is close to the diffusion-limited value as expected from the exergonic electron transfer. Photoinduced electron transfer from Ph_3P to $^1AcrH^+*$ also occurs to yield $Ph_3P^{\bullet+}$, which reacts with O_2. The rate constant of the reaction of $Ph_3P^{\bullet+}$ with O_2 was determined to be $1.5 \times 10^5\ M^{-1}\ s^{-1}$.[138]

The mechanism of the photocatalytic oxygenation of Ph_3P by O_2 with Acr^+–Mes is shown in Scheme 12. Triphenylphosphine peroxide (Ph_3PO_2) is produced via addition of O_2 to $Ph_3P^{\bullet+}$ to give Ph_3P peroxide radical cation ($Ph_3PO_2^{\bullet+}$), which undergoes back electron transfer from $Acr^{\bullet}$–Mes to $Ph_3PO_2^{\bullet+}$ (reaction pathway A in Scheme 12) and via radical coupling between $Ph_3P^{\bullet+}$ and $O_2^{\bullet-}$ (reaction pathway B in Scheme 12). Ph_3PO_2 reacts with Ph_3P to produce $Ph_3P{=}O$ via O–O bond cleavage.[139,140]

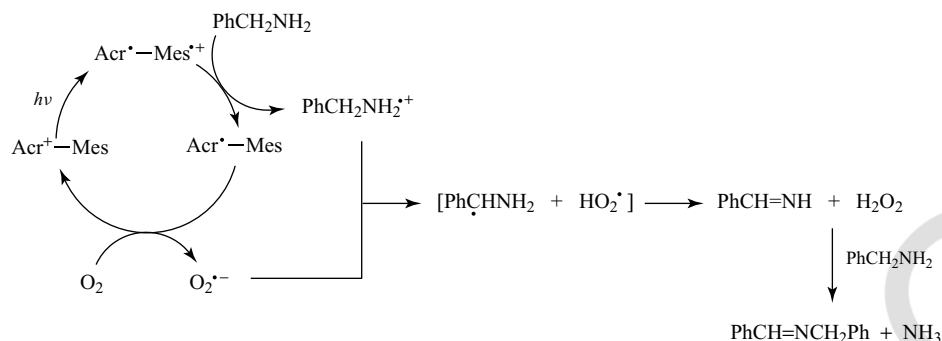## 3.5   Photocatalytic Oxidation of Benzylamine

Benzylamine is also oxidized by the photogenerated electron-transfer state of Acr^+–Mes in O_2-saturated MeCN to yield N-benzylidenebenzylamine, $PhCH_2N{=}CHPh$.[137] The reaction mechanism of the photocatalytic oxidation of benzylamine by O_2 with Acr^+–Mes is shown in Scheme 13.[137] The photogenerated electron-transfer state of Acr^+–Mes ($Acr^{\bullet}$–$Mes^{\bullet+}$) oxidizes benzylamine and reduces O_2 by electron transfer to produce the benzylamine radical cation and $O_2^{\bullet-}$, respectively. The subsequent proton transfer occurs from benzylamine radical cation to $O_2^{\bullet-}$ to give the α-hydrogen abstracted radical of benzylamine and hydrogen peroxyl radical ($HO_2^{\bullet}$). The α-hydrogen abstracted radical spontaneously reacts with $HO_2^{\bullet}$ to form benzylimine ($PhCH{=}NH$) and hydrogen peroxide (H_2O_2). $PhCH{=}NH$ reacts with benzylamine to produce the primary product $PhCH_2N{=}CHPh$ (Scheme 13).[141–143]

3.6   Photocatalytic Oxidation and Cleavage of DNA

Photoinduced DNA cleavage has attracted considerable interest because of the biological significance of DNA damage and repair (see **Oxidatively Generated Nucleobase Modifications in Isolated and Cellular DNA**, Volume 3 and **Oxidatively Formed Sugar Radicals in Nucleic Acids**,

rad038

rad039
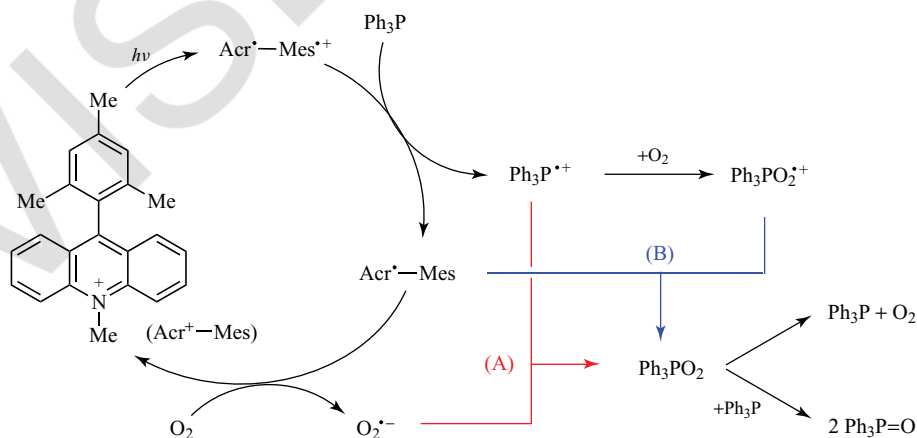
Scheme 12   Photocatalytic oxygenation of Ph_3P by O_2 with Acr^+–Mes.[137]

Scheme 13 Photocatalytic oxidation of benzylamine by O_2 with Acr^+–Mes.[137]

Volume 3).[144–149] The DNA cleavage resulted from efficient electron-transfer oxidation by the electron-transfer state of Acr^+–Mes.[150,151] The reduction potential of $Acr^•$–$Mes^{•+}$ ($E_{red} = 2.06$ V vs SCE in MeCN)[134] is much more positive than the one-electron oxidation potential of guanosine-5′-monophosphate (GMP, $E_{ox} = 1.07$ V vs SCE in an aqueous solution).[152] Thus, electron transfer from GMP to the $Mes^{•+}$ moiety of $Acr^•$–$Mes^{•+}$ is energetically feasible.[150] Formation of GMP radical cation ($GMP^{•+}$: $\lambda_{max} = 510$ nm) is observed by the laser photoirradiation of a buffer solution of Acr^+–Mes at pH 2.0 containing GMP as shown in Figure 10a (closed rectangles).[150] At pH 7.0, a transient absorption at the long wavelength region circa at 650 nm appears because of the deprotonation of $GMP^{•+}$ (closed circles in Figure 10a).[153,154] The difference spectra given in Figure 10b, obtained by subtracting the spectra in the absence of GMP from those in the presence of GMP at pH 2.0 and 7.0, correspond to those between $GMP^{•+}$ (positive absorption) and the $Mes^{•+}$ moiety (negative absorption), because the spectra in the absence and the presence of GMP are those of $Acr^•$–$Mes^{•+}$ and those of $GMP^{•+}$ and $Acr^•$–Mes, respectively.[150] The rate of formation of $GMP^{•+}$ obeyed pseudo-first-order kinetics and the pseudo-first-order rate constant increased linearly with increasing concentration of GMP at pH 2.0.[150] The second-order rate constant (k_{et}) of electron transfer from GMP to the $Mes^{•+}$ moiety of $Acr^•$–$Mes^{•+}$ was determined to be 4.3×10^7 M^{-1} s^{-1} in the buffer solution at 298 K.[150] The k_{et} value of electron transfer from GMP to the $Mes^{•+}$ moiety of $Acr^•$–$Mes^{•+}$ was also determined to be 2.7×10^8 M^{-1} s^{-1} at pH 7.0, which is much larger

than the value (4.3×10^7 M^{-1} s^{-1}) at pH 2.0, but still smaller than the diffusion limit.[150] The larger k_{et} value at the higher pH indicates the involvement of deprotonation associated with electron transfer (proton-coupled electron transfer).[155,156]

The transient absorption spectrum of oxidized DNA shown in Figure 11 is similar to that of $GMP^{•+}$ in Figure 10.[150] The k_{et} value of the electron-transfer oxidation of DNA was determined to be 4.8×10^7 M^{-1} s^{-1}, which is larger than the k_{et} value of GMP.[150] The electron-transfer oxidation of DNA results in the cleavage of DNA.[150] The DNA cleavage activity with Acr^+–Mes in the absence of O_2 was much higher than that in the presence of O_2 at pH 5.0 and 7.0.[150] This indicates that O_2 acts as an apparent inhibitor for the DNA cleavage. When DNA is oxidized by the $Mes^{•+}$ moiety of $Acr^•$–$Mes^{•+}$, O_2 is reduced by the $Acr^•$ moiety to produce $O_2^{•-}$.[78,150] The retarding effect of O_2 may result from more efficient back electron transfer from $O_2^{•-}$ to DNA radical cation as compared with that from the $Acr^•$ moiety to DNA radical cation before oxidizing DNA as shown in Scheme 14.[150]

Although all DNA bases can be oxidized by the $Mes^{•+}$ moiety of $Acr^•$–$Mes^{•+}$, the largest k_{et} value of the electron-transfer oxidation of GMP together with the lowest oxidation potential of GMP among DNA bases indicate that guanine is eventually oxidized in electron transfer from DNA to the $Mes^{•+}$ moiety of $Acr^•$–$Mes^{•+}$, leading to efficient DNA cleavage.[157] In the present case, however, no hydroxyl radical ($HO^•$) was formed because the photoexcitation of Acr^+–Mes affords the electron-transfer state, which oxidizes DNA without involvement of the triplet excited state.[158] The higher DNA cleavage activity at pH 5.0 as compared with that at pH 7.0 suggests
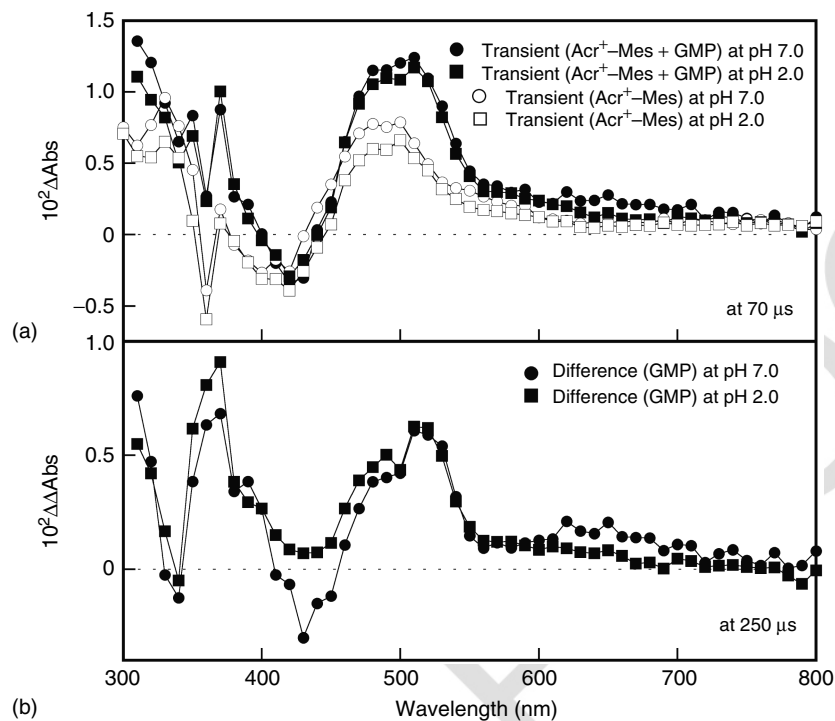
Figure 10   (a) Transient absorption spectra of Acr^+–Mes in the presence and absence of GMP $(1.0 \times 10^{-2}\,M)$ at pH 2.0 and 7.0; (b) difference transient absorption spectra of $GMP^{\bullet +}$ (pH 2.0) and $(GMP–H)^{\bullet}$ (pH 7.0), obtained by subtracting the spectra in the absence of GMP from those in the presence of GMP at pH 2.0 and 7.0, respectively.[150]
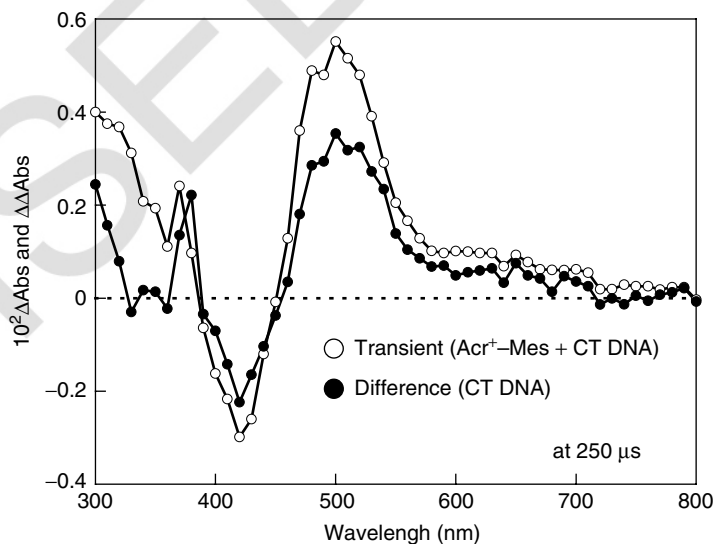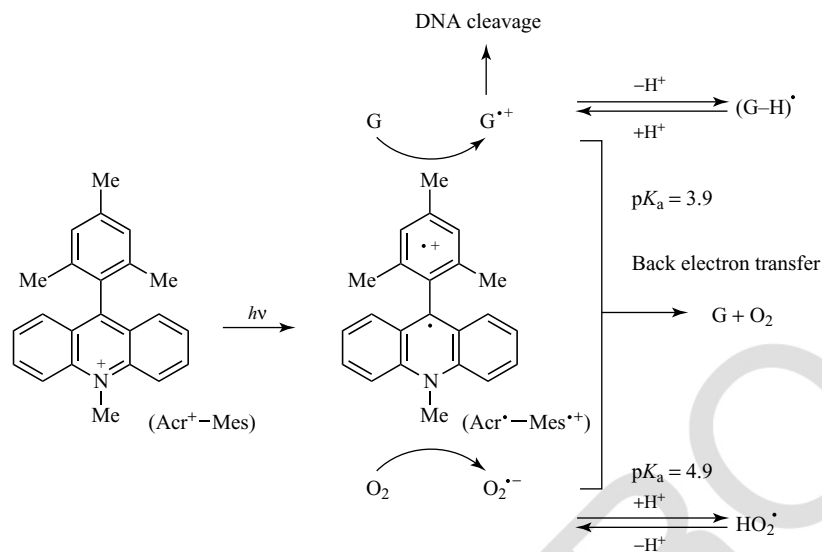

Figure 11   Transient absorption spectrum of Acr^+–Mes $(6.0 \times 10^{-5}\,M)$ in the presence of calf thymus DNA (CT DNA) $(1.0 \times 10^{-3}\,M)$ and the difference spectrum of DNA radical cation at pH 7.0 measured at 250 μs after laser excitation at $\lambda = 355\,nm$ at 298 K.[150]

Scheme 14 Photocatalytic oxidation and cleavage of DNA by O_2 with Acr^+–Mes.[150]

that guanine radical cation has a higher reactivity for the DNA cleavage than the deprotonated radical (Scheme 14), judging from the pK_a value of guanine radical cation ($pK_a = 3.9$).[154]
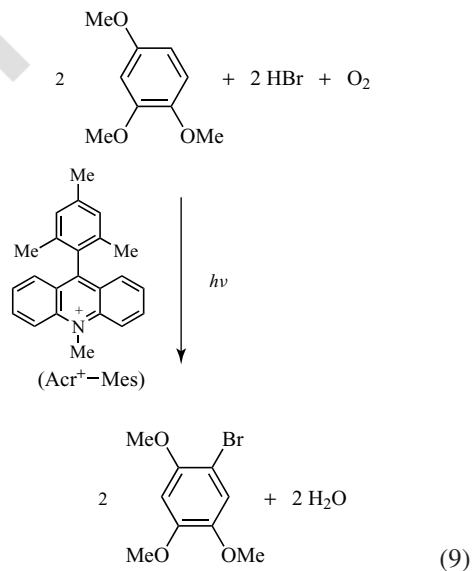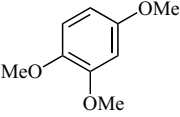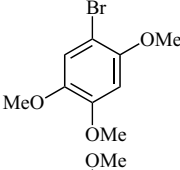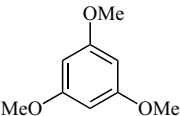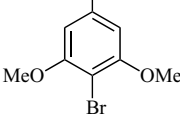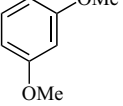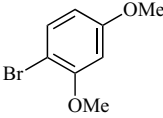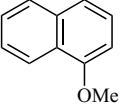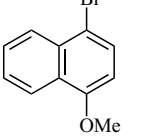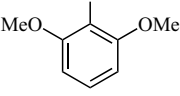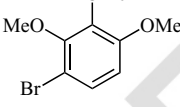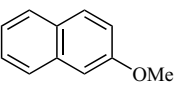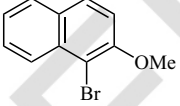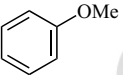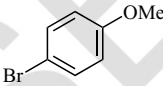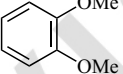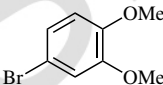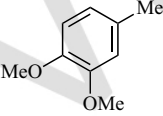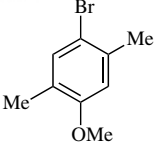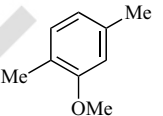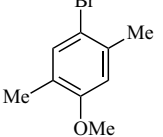
4   PHOTOCATALYTIC BROMINATION VIA CHARGE SEPARATION

Acr^+–Mes was found to act as an efficient photo-catalyst for selective bromination of aromatic hydro-carbons and thiophenes with aqueous HBr as a Br source without using a toxic bromine source and O_2 as a green oxidant under visible light irradiation.[159] It should be noted that bromination of thiophenes is particularly important in the preparation of olig-othiophenes and polythiophenes,[160–174] which have many applications as conductive, semiconductive, nonlinear optical, and liquid crystalline materials.[175]

Visible light irradiation of $[Acr^+$–Mes]$ClO_4{}^-$ ($\lambda_{max} = 430$ nm, 0.20 mM) in an oxygen-saturated MeCN solution containing 1,2,4-trimethoxybenzene (TMB, 4.0 mM), 50% aqueous HBr ([HBr] = 20 mM, [H_2O] = 100 mM) with a xenon lamp attached with UV-cut glass filter ($\lambda < 320$ nm) for 20 min resulted in formation of a brominated product, 2,4,5-trimethoxybromobenzene.[159] The overall stoi-chiometry of the photocatalytic reaction is given by

the following equation:

$$(9)$$

The yield and selectivity of 2,4,5-tri-methoxybromo-benzene is nearly 100%, because no further brominated product, dibromo- or tribromo-derivative, was produced in these reaction conditions.[159] The products and quantum yields are listed in Table 2.[159] Photocatalytic bromination reactions of various aromatic compounds also occurred as shown in Table 2. A preparative scale

Table 2 Product and quantum yields for photocatalytic bromination of organic compounds by O_2 and HBr with Acr^+–Mes in MeCN, and one-electron oxidation potentials of substrates.[159]

Entry	Substrate	Product	Conversion[a] (%)	Yield[a] (%)	Time (h)	Quantum yield[a] (%)	$E_{ox}{}^{b}$ (V)
1			>99	>99	0.3	4.3	0.96
2			>99	>99	0.3	4.8	1.43
3			>99	>99	0.3	3.9	1.49
4			>99	>99	0.5	3.1	1.34
5			>99	>99	1.5	1.1	1.42
6			>99	>99	2	0.26	1.47
7			>99	>99	16	0.01	1.76
8			>99	78[c]	3	0.10	1.45
9			>99	53	2	0.36	1.33
10			>99	44	2	0.32	1.47

[a] Conditions: [substrate] = 4.0 mM; [Acr^+–Mes] = 0.20 mM; [HBr] = 20 mM; [H_2O] = 100 mM.
[b] Values are determined by cyclic voltammetry and second harmonic ac voltammetry.
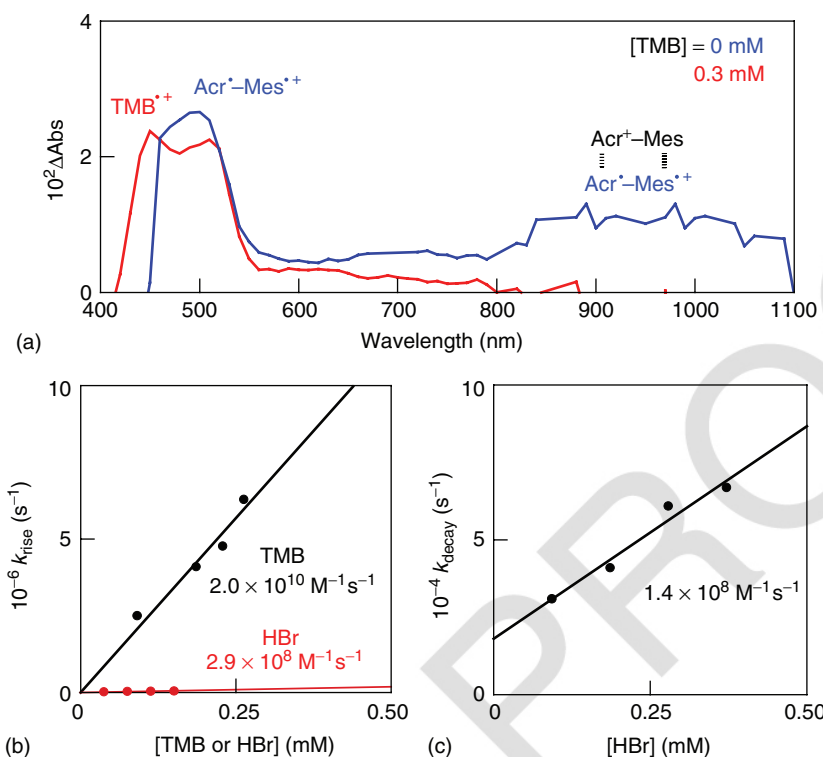[c] Minor product is mainly the dibromo compound.

Figure 12   (a) Transient absorption spectra of the electron-transfer state of Acr^+–Mes (0.2 mM) in the absence and presence of TMB (0.3 mM) in deaerated MeCN after nanosecond laser excitation at 430 nm. (b) Plot of k_{rise} versus [TMB] or [HBr] for the reaction of $Acr^•$–$Mes^{•+}$ with TMB or HBr. (c) Plot of k_{decay} versus [HBr] for the reaction of $TMB^{•+}$ with HBr.[159]

photocatalytic reaction of TMB (200 mg, 1.2 mmol) with 50% aqueous HBr (160 μl 1.5 mmol) in the presence of Acr^+–Mes (0.044 mmol) in an oxygen-saturated MeCN under photoirradiation by a xenon lamp for 24 h affords the brominated product in 100% selectivity and in 81% yield.[159]

The photodynamics of the photocatalytic bromination of TMB with HBr in the presence of Acr^+–Mes was revealed by nanosecond laser flash photolysis.[159] A transient absorption spectrum due to the electron-transfer state of Acr^+–Mes ($Acr^•$–$Mes^{•+}$) is observed after the laser pulse excitation at 430 nm of an MeCN solution of Acr^+–Mes as shown in Figure 12 (blue line).[159] The broad absorption band in the NIR region is attributed to the π-dimer of $Acr^•$–$Mes^{•+}$ with the ground state of Acr^+–Mes as described earlier.[55] In the presence of TMB, a new band at 450 nm appeared at 12 μs as shown in Figure 12 (red line), which is assigned to TMB radical cation ($TMB^{•+}$).[159] The rate constant for electron transfer from TMB to the

$Mes^{•+}$ at the electron-transfer state of Acr^+–Mes was determined from the slope of the linear plot of k_{rise} versus [TMB] to be $k_{TMB} = 2.0 \times 10^{10}$ M^{-1} s^{-1} (Figure 12b).[159] The rate of disappearance of $TMB^{•+}$ was accelerated by increasing the concentration of HBr.[159] The observed decay rate constant (k_{decay}) increases linearly with increasing concentrations of HBr as shown in Figure 12c.[159] Thus, $TMB^{•+}$ efficiently reacts with Br^- to form the Br adduct radical [$TMB(Br)^•$]. The rate constant of the addition of Br^- was determined from the slope of k_{decay} versus [HBr] to be $k_{HBr} = 1.4 \times 10^8$ M^{-1} s^{-1} (Figure 12c).[159] The electron-transfer oxidation of Br^- in the photocatalytic reaction was also revealed by quenching of $Acr^•$–$Mes^{•+}$ by HBr. The quenching rate constant of $Acr^•$–$Mes^{•+}$ with HBr is two orders of magnitude smaller (2.9×10^8 M^{-1} s^{-1}) than the k_{TMB} value (Figure 12b).[159] Thus, the electron-transfer oxidation of hexamethylbenzene (HMB) predominated over the oxidation of Br^-.

The one-electron oxidation potentials (E_{ox}) of aromatic compounds in deaerated MeCN (0.96–1.76 V) listed in Table 2 are lower than the one-electron reduction potential of the electron-transfer state of Acr$^+$–Mes (Acr$^\bullet$–Mes$^{\bullet+}$; $E_{red} = 2.06$ V vs SCE).[134,159] Thus, electron transfer from aromatic compounds such as TMB to Acr$^\bullet$–Mes$^{\bullet+}$ is energetically favorable, whereas electron transfer from toluene ($E_{ox} = 2.20$ V) and benzene (2.32 V) to the Mes$^{\bullet+}$ moiety of Acr$^\bullet$–Mes$^{\bullet+}$ is energetically unfavorable. In such a case, no photocatalytic bromination of benzene or toluene occurs under the same experimental conditions as TMB. The decreased reactivity of methoxybenzene (entry 7 in Table 2) is attributed to the high E_{ox} value (1.76 V). On the other hand, the one-electron reduction of O_2 by the electron-transfer state of Acr$^+$–Mes in the presence of an acid is known to occur efficiently, producing HO$_2^\bullet$ that disproportionates to yield H_2O_2 and O_2.[176] The rate constant of electron-transfer reduction of O_2 (k_{O_2}) was reported to be 6.8×10^8 M^{-1} s^{-1}.[134]

The photocatalytic bromination of TMB by HBr with Acr$^+$–Mes is initiated by intramolecular photoinduced electron transfer from the Mes moiety to the singlet excited state of the Acr$^+$ moiety of Acr$^+$–Mes to generate Acr$^\bullet$–Mes$^{\bullet+}$ as shown in Scheme 15.[44,159]

The Mes$^{\bullet+}$ moiety of Acr$^\bullet$–Mes$^{\bullet+}$ can oxidize TMB to produce TMB$^{\bullet+}$, whereas the Acr$^\bullet$ moiety can reduce O_2 to HO$_2^\bullet$.[159] The TMB$^{\bullet+}$ thus produced reacts with Br$^-$ to form the Br adduct radical, which undergoes dehydrogenation with protonated HO$_2^\bullet$ to afford the corresponding brominated product and hydrogen peroxide.[159] Hydrogen peroxide further reacts with HBr and substrate to produce another brominated product and H_2O.[177] The quantum yield remained constant on increasing the concentration of TMB and the light intensity under the present experimental conditions.[159] This suggests that no radical chain process is involved in the present photocatalytic aerobic bromination of substrates with HBr.

5 CARBON–CARBON BOND FORMATION VIA CHARGE SEPARATION

5.1 Oligomerization of Fullerene

Because the photogenerated electron-transfer state of Acr$^+$–Mes (Acr$^\bullet$–Mes$^{\bullet+}$) has both the highly oxidizing and reducing ability, the same substrate (S) can be oxidized and reduced by Acr$^\bullet$–Mes$^{\bullet+}$ to produce the radical cation (S$^{\bullet+}$) and the radical anion (S$^{\bullet-}$), which can be coupled to yield the dimer (S–S). Such an example has been reported for the coupling of fullerene radical cation ($C_{60}^{\bullet+}$) and fullerene radical anion ($C_{60}^{\bullet-}$), which are produced by electron-transfer oxidation and reduction of C_{60} with Acr$^\bullet$–Mes$^{\bullet+}$ as shown in Scheme 16.[178] The coupling products were fullerene oligomers, C_{120}, C_{180}, and C_{240}.[178]

Nanosecond laser excitation at 430 nm of a deaerated PhCN solution containing Acr$^+$–Mes and C_{60} results in the appearance of new transient absorption bands in the NIR region, which are the superposition of those due to $C_{60}^{\bullet+}$ (960 nm) and $C_{60}^{\bullet-}$ (1080 nm) as shown in Figure 13a.[178–180] The transient absorption bands of $C_{60}^{\bullet+}$ and $C_{60}^{\bullet-}$ disappear, accompanied by appearance of a new absorption band at 740 nm due to the triplet excited
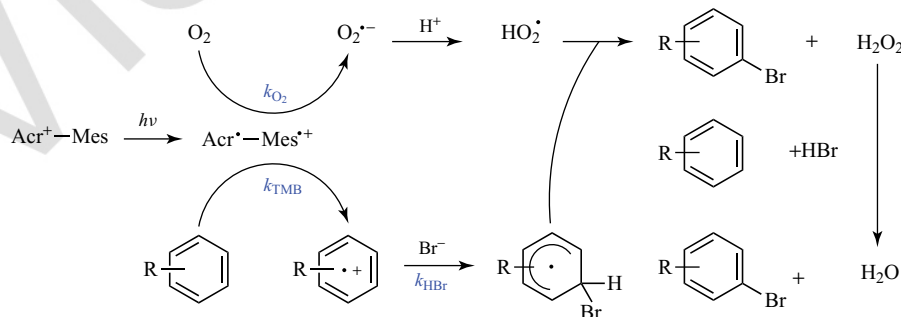
Scheme 15   Photocatalytic bromination of alkylbenzenes by HBr and O_2 with Acr$^+$–Mes.[159]
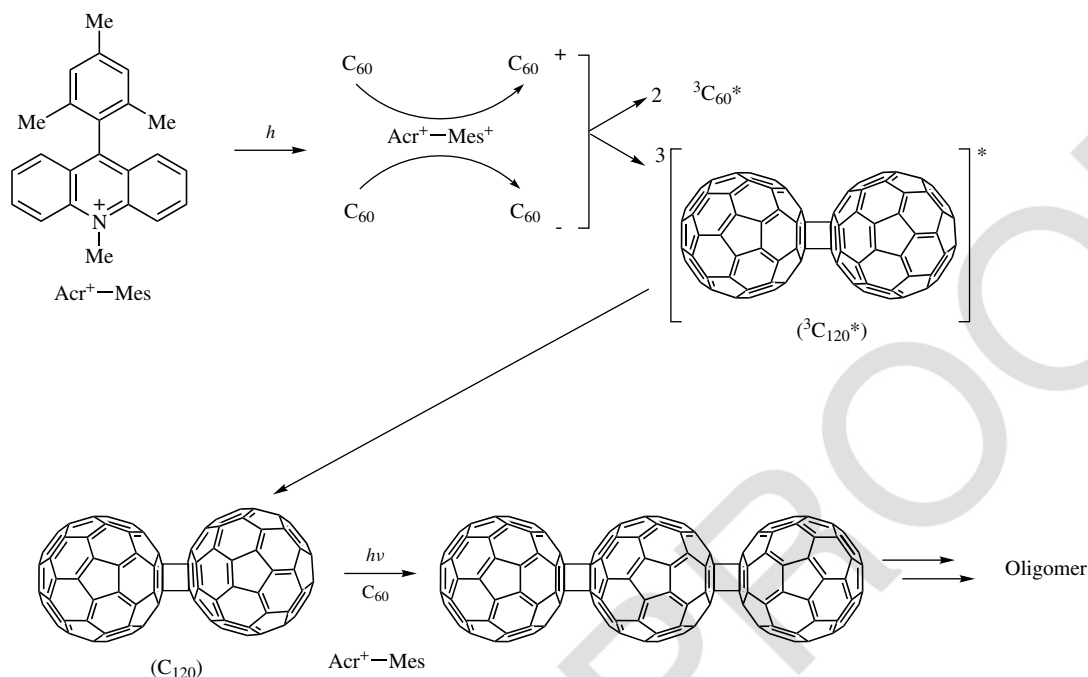
Scheme 16   Photocatalytic oligomerization of fullerene with Acr$^+$–Mes.[178]
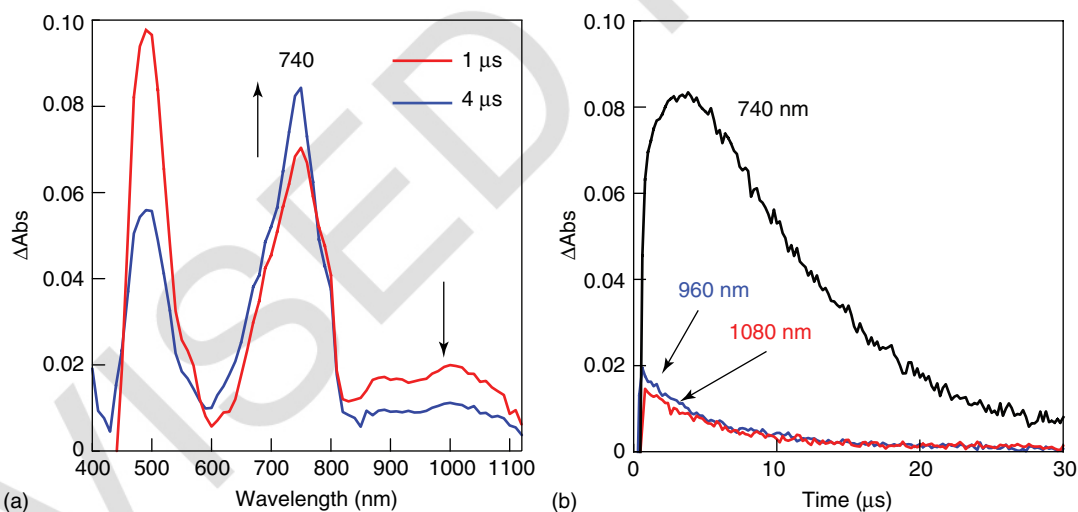
Figure 13   (a) Transient absorption spectra in PhCN observed in photoinduced electron-transfer oxidation of C$_{60}$ (1.0×10^{-4} M) with Acr$^+$–MesClO$_4^-$ (1.0×10^{-4} M) taken 1.0 and 4.0 μs after laser excitation at 430 nm at 298 K. (b) Time profiles at 740, 960, and 1080 nm in PhCN.[178]

state of C$_{60}$ (^{3}C$_{60}$*) (Figure 13b). The reaction mechanism of photoinduced oligomerization of C$_{60}$ with Acr$^+$–Mes is summarized in Scheme 16, where only a linear isomer is shown for C$_{180}$.[178]

Because the free energy change of electron transfer (ΔG_{et}) from C$_{60}$ ($E_{ox} = 1.73$ V vs SCE)[180,181] to the Mes$^{•+}$ moiety of the electron-transfer state of Acr$^+$–Mes in PhCN ($E_{ox} = 1.88$ V)[44,78] is negative

($\Delta G_{et} = -0.15$ eV), the electron-transfer oxidation C_{60} is energetically feasible to form $C_{60}^{\bullet+}$. On the other hand, the electron-transfer reduction of C_{60} ($E_{red} = -0.43$ V)[182] with the Acr$^\bullet$ moiety ($E_{red} = -0.49$ V)[44,78] is also thermodynamically feasible to give $C_{60}^{\bullet-}$ ($\Delta G_{et} = -0.06$ eV). Thus, C_{60} acts as both an electron donor and acceptor in electron-transfer reactions of Acr$^\bullet$–Mes$^{\bullet+}$ with C_{60} to produce $C_{60}^{\bullet+}$ and $C_{60}^{\bullet-}$ at the same time. The $[2+2]$cycloaddition occurs efficiently between $C_{60}^{\bullet+}$ and $C_{60}^{\bullet-}$ to afford $^3C_{120}^*$ rather than C_{120}, because the driving force of charge recombination (2.16 eV) is larger than the triplet excited state energy of C_{120} (circa 1.5 eV).[178,183] The radical coupling between $C_{60}^{\bullet-}$ and $C_{60}^{\bullet+}$ also affords the triplet excited state of C_{60} ($^3C_{60}^*$). Further oligomerization occurs by the same process.

5.2 Photocatalytic Dimerization of Anthracene

Photodimerization of anthracene is made possbile using Acr$^+$–Mes as a photocatalyst in CHCl$_3$.[184] When the photochemical reaction of 9,10-dimethylanthracene with Acr$^+$–Mes was carried out without O$_2$ in CHCl$_3$, photocatcalytic carbon–carbon bond formation occurred efficiently to give dimethyllepidopterene (5,6,11,12-tetrahydro-5,12-dimethyl-4b,12[1′,2′]: 6,10b[1″,2″]-dibenzochrysene).[184] The X-ray crystal structure of dimethyllepidopterene is shown in Figure 14.[184] In the crystal structure, the bond length of the newly formed C–C bond (C6–C6′) is 1.629(2) Å, which is much longer than normal C–C single bonds, indicating severe distortion of this compound.[184] The synthesis of another type of anthracene dimer such as lepidopterene has previously been carried out by intramolecular Diels–Alder reaction of 9-anthrylmethyl a,p-dimer,[185–189] dehalogenation of 9-chloromethylanthracene,[190,191] oxidation of 9-methylanthracene with copper(II)/peroxy-disulfate,[192] photolysis of 9-(N,N-dimethylamino)-anthracene,[193] 9-(phenoxymethyl)anthracene,[194] and 9-anthrcenylmethylsulfides and selenides.[195]

The one-pot synthesis of the lepidopterene from the corresponding anthracene has been made possbile using Acr$^+$–Mes as a photocatalyst as shown in Scheme 17.[184] Photoirradiation of Acr$^+$–Mes
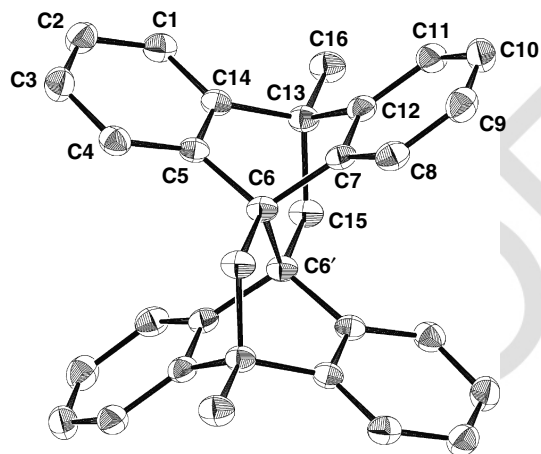
Figure 14 Crystal structure of dimethyllepidopterene produced in the Acr$^+$–Mes-catalyzed photochemical reaction of DMA.[184]

affords the electron-transfer state (Acr$^\bullet$–Mes$^{\bullet+}$), followed by electron transfer from DMA to Acr$^\bullet$–Mes$^{\bullet+}$ to produce DMA$^{\bullet+}$ and Acr$^\bullet$–Mes. The deprotonation from the methyl group of DMA$^{\bullet+}$ is the key step for the formation of dimethyllepidopterene as shown in Scheme 17. There are two ways of radical coupling of the deprotnated radicals to produce the dimers: lepidopterene and 1,2-bis(9-anthracenyl)ethane (Scheme 17). The Acr$^\bullet$ moiety of Acr$^\bullet$–Mes, produced by electron transfer from DMA to Acr$^\bullet$–Mes$^{\bullet+}$, is oxidized by dissociative electron transfer to CHCl$_3$ to produce CHCl$_2^\bullet$ and Cl$^-$. The CHCl$_2^\bullet$ radicals dimerize to yield 1,1,2,2-tetrachloroethane (CHCl$_2$CHCl$_2$) as shown in Scheme 17.[184]

The improvement of the dimer product yield can be achieved by the addition of a base such as tetrabutylammonium hydroxide (TBAOH), which accelerates deprotonation of DMA$^{\bullet+}$.[184] When TBAOH was introduced to a CHCl$_3$ solution containing DMA and Acr$^+$–Mes, the isolated yield of dimethyllepidopterene was increased to 21%, as compared with the yield in the absence of the base (12%).[184]

6 SUMMARY

As described above, a variety of photocatalytic reactions are made possible using the electron-transfer state of Acr$^+$–Mes, which can oxidize and reduce
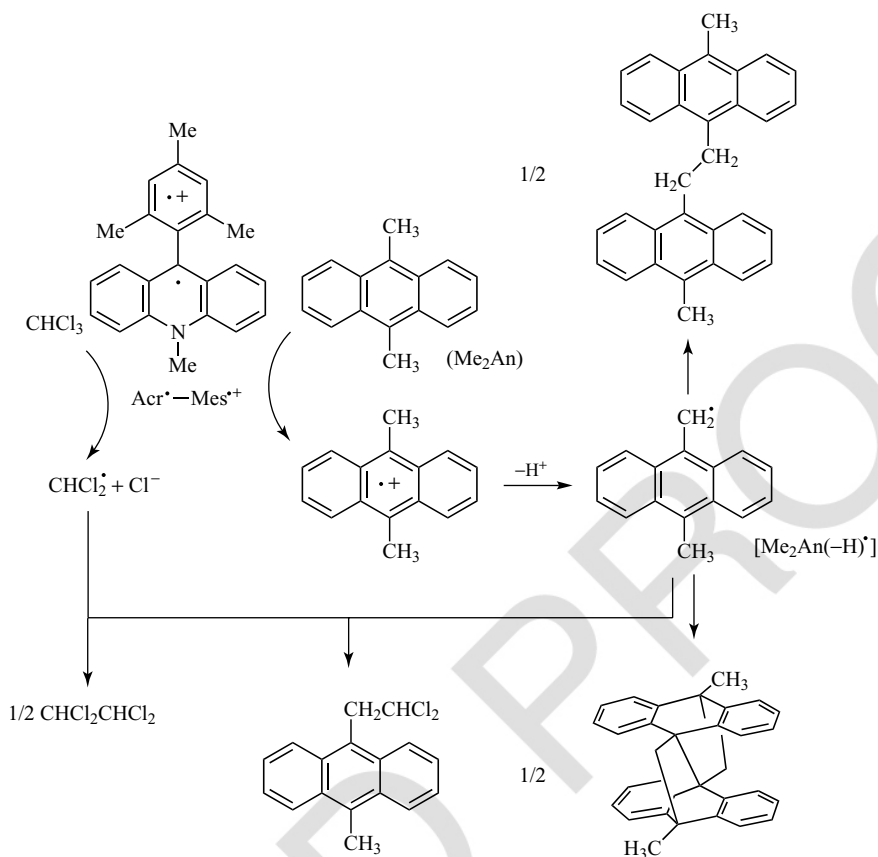
Scheme 17 Photocatalytic formation of dimethyllepidopterene with Acr$^+$–Mes.[184]

external electron donors and acceptors to produce the radical cations and anions, respectively. The reactions of radical cations with superoxide anion ($O_2{}^{\bullet-}$) can efficiently compete with the back electron transfer to yield the oxygenated products. Substrates that cannot react with singlet oxygen can be readily oxygenated by oxygen with Acr$^+$–Mes under visible light irradiation. The oxygenated products become much more difficult to be oxidized by the electron-transfer state of Acr$^+$–Mes, when the selective photocatalytic oxygenation of substrates, which would otherwise be very difficult to achieve, has been made possible with Acr$^+$–Mes. The reactions of radical cations produced by electron transfer from electron donor substrates to the electron-transfer state of Acr$^+$–Mes with nucleophiles such as Br$^-$ can also afford the adducts with nucleophiles, when the electron-transfer oxidation of substrates with the electron-transfer state

of Acr$^+$–Mes is much faster than that of nucleophiles. In addition, the radical coupling of neutral radicals produced by deprotonation of the produced radical cations can be utilized for the C–C bond formation reactions. Thus, photocatalytic reactions of Acr$^+$–Mes under visible light irradiation provide new ways to design environmentally benign synthesis.

REFERENCES

1. J. Fossey, D. Lefort, and J. Sorba, *Free Radicals in Organic Chemistry*, Wiley, New York, 1995.
2. B. Giese, *Radicals in Organic Synthesis. Formation of Carbon-Carbon Bonds*, ed. J. E. Baldwin, Pergamon Press, Oxford, 1986.
3. P. Renaoud and M. P. Sibi, eds., *Radicals in Organic Synthesis*, Wiley-VCH, Weinheim, 2001, vol. 2.

4. H. Togo, *Advanced Free Radical Reactions for Organic Synthesis*, Elsevier, Amsterdam, 2004.

5. F. Minisci, ed., *Free Radicals in Biology and Environment*, Kluwer, Dordrecht, 1997.

6. M. Schmittel and M. K. Ghorai, in *Electron Transfer in Chemistry*, ed. V. Balzani, Wiley-VCH, Weinheim, 2001, vol. 2, pp. 5–54.

7. L. Eberson, *Electron Transfer Reactions in Organic Chemistry, Reactivity and Structure*, Springer, Heidelberg, 1987, vol. 25.

8. S. Fukuzumi, in *Advances in Electron Transfer Chemistry*, ed. P. S. Mariano, JAI Press, Greenwich, 1992, vol. 2, pp. 67–175.

9. S. Fukuzumi, in *Electron Transfer in Chemistry*, ed. V. Balzani, Wiley-VCH, Weinheim, 2001, vol. 4, pp. 3–67.

10. S. Das and V. Suresh, in *Electron Transfer in Chemistry*, ed. V. Balzani, Wiley-VCH, Weinheim, 2001, vol. 2, pp. 379–456.

11. S. Fukuzumi, K. Ohkubo, and T. Okamoto, *J. Am. Chem. Soc.*, 2002, **124**, 14147–14155.

12. S. Fukuzumi, Y. Fujii, and T. Suenobu, *J. Am. Chem. Soc.*, 2001, **123**, 10191–10199.

13. C. Amatore and A. R. Brown, *J. Am. Chem. Soc.*, 1996, **118**, 1482–1486.

14. S. Fukuzumi, *Org. Biomol. Chem.*, 2003, **1**, 609–620.

15. S. Fukuzumi, *Pure Appl. Chem.*, 2007, **79**, 981–991.

16. G. Palmisano, V. Augugliaro, M. Pagliaro, and L. Palmisano, *Chem. Commun.*, 2007, 3425–3437.

17. S. Fukuzumi, *Bull. Chem. Soc. Jpn.*, 2006, **79**, 177–195.

18. R. E. Galian and J. Pérez-Prieto, *Energy Environ. Sci.*, 2010, **3**, 1488–1498.

19. D. Gust, T. A. Moore, and A. L. Moore, in *Electron Transfer in Chemistry*, ed. V. Balzani, Wiley-VCH, Weinheim, 2001, vol. 3, pp. 272–336.

20. D. Gust and T. A. Moore, in *The Porphyrin Handbook*, eds. K. M. Kadish, K. M. Smith, and R. Guilard, Academic Press, San Diego, CA, 2000, vol. 8, pp. 153–190.

21. D. Gust, T. A. Moore, and A. L. Moore, *Acc. Chem. Res.*, 2001, **34**, 40–48.

22. M. R. Wasielewski, *Chem. Rev.*, 1992, **92**, 435–461.

23. M. P. Debreczeny, W. A. Svec, and M. R. Wasielewski, *Science*, 1996, **274**, 584–587.

24. A. Osuka, N. Mataga, and T. Okada, *Pure Appl. Chem.*, 1997, **69**, 797–802.

25. K. D. Jordan and M. N. Paddon-Row, *Chem. Rev.*, 1992, **92**, 395–410.

26. M. N. Paddon-Row, *Acc. Chem. Res.*, 1994, **27**, 18–25.

27. J. W. Verhoeven, *Adv. Chem. Phys.*, 1999, **106**, 603–644.

28. M. N. Paddon-Row, *Adv. Phys. Org. Chem.*, 2003, **38**, 1–85.

29. M.-J. Blanco, M. Consuelo Jiménez, J.-C. Chambron, *et al.*, *Chem. Soc. Rev.*, 1999, **28**, 293–305.

30. J.-C. Chambron, J.-P. Collin, J.-O. Dalbavie, *et al.*, *Coord. Chem. Rev.*, 1998, **178–180**, 1299–1312.

31. A. Harriman and J.-P. Sauvage, *Chem. Soc. Rev.*, 1996, **25**, 41–47.

32. S. Fukuzumi and D. M. Guldi, in *Electron Transfer in Chemistry*, ed. V. Balzani, Wiley-VCH, Weinheim, 2001, vol. 2, pp. 270–337.

33. S. Fukuzumi and T. Kojima, *J. Mater. Chem.*, 2008, **18**, 1427–1439.

34. S. Fukuzumi, T. Honda, K. Ohkubo, and T. Kojima, *Dalton Trans.*, 2009, 3880–3889.

35. F. D. Lewis, R. L. Letsinger, and M. R. Wasielewski, *Acc. Chem. Res.*, 2001, **34**, 159–170.

36. H. Imahori, K. Tamaki, D. M. Guldi, *et al.*, *J. Am. Chem. Soc.*, 2001, **123**, 2607–2617.

37. H. Imahori, D. M. Guldi, K. Tamaki, *et al.*, *J. Am. Chem. Soc.*, 2001, **123**, 6617–6628.

38. S. Fukuzumi, K. Ohkubo, H. Imahori, *et al.*, *J. Am. Chem. Soc.*, 2001, **123**, 10676–10686.

39. K. Ohkubo, H. Imahori, J. Shao, *et al.*, *J. Phys. Chem. A*, 2002, **106**, 10991–10998.

40. Y. Kashiwagi, K. Ohkubo, J. A. MacDonald, *et al.*, *Org. Lett.*, 2003, **5**, 2719–2712.

41. S. Fukuzumi, *Phys. Chem. Chem. Phys.*, 2008, **10**, 2283–2297.

42. S. Fukuzumi, K. Ohkubo, T. Suenobu, *et al.*, *J. Am. Chem. Soc.*, 2001, **126**, 8459–8467.

43. K. Kikuchi, M. Watabe, H. Ikeda, *et al.*, *J. Am. Chem. Soc.*, 1993, **115**, 5180–5184.

44. S. Fukuzumi, H. Kotani, K. Ohkubo, *et al.*, *J. Am. Chem. Soc.*, 2004, **126**, 1600–1601.

45. A. Harriman, *Angew. Chem. Int. Ed.*, 2004, **43**, 4985–4987.

46. K. Ohkubo, H. Kotani, and S. Fukuzumi, *Chem. Commun.*, 2005, 4520–4522.

47. J. W. Verhoeven, H. J. van Ramesdonk, M. M. Groeneveld, *et al.*, *ChemPhysChem*, 2005, **6**, 2251–2260.

48. A. C. Benniston, A. Harriman, P. Li, *et al.*, *Chem. Commun.*, 2005, 2701–2702.

49. A. C. Benniston, A. Harriman, P. Li, *et al.*, *J. Am. Chem. Soc.*, 2005, **127**, 16054–16064.

50. A. C. Benniston, A. Harriman, and J. W. Verhoeven, *Phys. Chem. Chem. Phys.*, 2008, **10**, 5156–5158.

51. A. C. Benniston, K. J. Elliott, R. W. Harrington, and W. Clegg, *Eur. J. Org. Chem.*, 2009, 253–258.

52. G. Jones II, M. S. Farahat, S. R. Greenfield, *et al.*, *Chem. Phys. Lett.*, 1994, **229**, 40–46.

53. H. van Willigen, G. Jones II, and M. S. Farahat, *J. Phys. Chem.*, 1996, **100**, 3312–3316.

54. G. Jones II, D.-X. Yan, S. R. Greenfield, *et al.*, *J. Phys. Chem. A*, 1997, **101**, 4939–4942.

55. S. Fukuzumi, H. Kotani, and K. Ohkubo, *Phys. Chem. Chem. Phys.*, 2008, **10**, 5159–5162.

56. N. Periasamy, *Chem. Phys. Lett.*, 1983, **99**, 322–325.

57. K. Kasama, K. Kikuchi, S. Yamamoto, *et al.*, *J. Phys. Chem.*, 1981, **85**, 1291–1296.

58. O. Morawski and J. Prochorow, *Chem. Phys. Lett.*, 1995, **242**, 253–258.

59. O. W. Howarth and G. K. Fraenkel, *J. Am. Chem. Soc.*, 1966, **88**, 4514–4515.

60. J. K. Kochi, R. Rathore, and P. L. Magueres, *J. Org. Chem.*, 2000, **65**, 6826–6836.

61. S. Fukuzumi, Y. Endo, and H. Imahori, *J. Am. Chem. Soc.*, 2002, **124**, 10974–10975.

62. J.-M. Lü, S. V. Rosokha, and J. K. Kochi, *J. Am. Chem. Soc.*, 2003, **125**, 12161–12171.

63. J. J. Novoa, P. Lafuente, R. E. Del Sesto, and J. S. Miller, *Angew. Chem. Int. Ed.*, 2001, **40**, 2540–2545.

64. R. E. Del Sesto, J. S. Miller, P. Lafuente, and J. J. Novoa, *Chem. Eur. J.*, 2002, **8**, 4894–4908.

65. J. Yuasa, T. Suenobu, and S. Fukuzumi, *J. Am. Chem. Soc.*, 2003, **125**, 12090–12091.

66. J. Yuasa and S. Fukuzumi, *J. Am. Chem. Soc.*, 2007, **129**, 12912–12913.

67. S. Fukuzumi, R. Hanazaki, H. Kotani, and K. Ohkubo, *J. Am. Chem. Soc.*, 2010, **132**, 11002–11003.

68. T. Hasobe, S. Hattori, H. Kotani, *et al*., *Org. Lett.*, 2004, **6**, 3103–3106.

69. N. Mizoshita, K. Yamanaka, T. Shimada, *et al*., *Chem. Commun.*, 2010, **46**, 9235–9237.

70. F. Hoffmann, M. Cornelius, J. Morell, and M. Fröba, *Angew. Chem. Int. Ed.*, 2006, **45**, 3216–3251.

71. M. Beretta, J. Morell, P. Sozzani, and M. Fröba, *Chem. Commun.*, 2010, **46**, 2495–2497.

72. T. P. Nguyen, P. Hesemann, P. Gaveau, and J. J. E. Moreau, *J. Mater. Chem.*, 2009, **19**, 4164–4171.

73. N. Mizoshita, Y. Goto, M. P. Kapoor, *et al*., *Chem. Eur. J.*, 2009, **15**, 219–226.

74. S. Inagaki, O. Ohtani, Y. Goto, *et al*., *Angew. Chem. Int. Ed.*, 2009, **48**, 4042–4046.

75. N. Mizoshita, M. Ikai, T. Tani, and S. Inagaki, *J. Am. Chem. Soc.*, 2009, **131**, 14225–14227.

76. M. Ohashi, M. Aoki, K. Yamanaka, *et al*., *Chem. Eur. J.*, 2009, **15**, 13041–13046.

77. H. Takeda, M. Ohashi, T. Tani, *et al*., *Inorg. Chem.*, 2010, **49**, 4554–4559.

78. H. Kotani, K. Ohkubo, and S. Fukuzumi, *J. Am. Chem. Soc.*, 2004, **126**, 15999–16006.

79. K. Ohkubo, T. Nanjo, and S. Fukuzumi, *Org. Lett.*, 2005, **7**, 4265–4268.

80. G. B. Schuster, *Acc. Chem. Res.*, 1979, **12**, 366–373.

81. E. S. Vysotski and J. Lee, *Acc. Chem. Res.*, 2004, **37**, 405–415.

82. H. Isobe, Y. Takano, M. Okumura, *et al*., *J. Am. Chem. Soc.*, 2005, **127**, 8667–8679.

83. C. S. Foote, J. S. Valentine, A. Greenberg, and J. F. Liebman, in *Active Oxygen*, eds., Blackie Academic and Professional, New York, 1995, vol. 2.

84. W. Adam, in *Four-Membered Ring Peroxides: 1,2-Dioxetanes and -Peroxylactones, The Chemistry of Peroxides*, ed. S. Patai, John Wiley & Sons, Ltd., New York, 1983, chap. 24, pp. 829–920.

85. A. Mayer and S. Neuenhoefer, *Angew. Chem. Int. Ed. Engl.*, 1994, **33**, 1044–1072.

86. W. Adam, D. Reinhardt, and C. R. Saha-Möller, *Analyst*, 1996, **121**, 1527–1531.

87. T. Wilson and A. P. Schaap, *J. Am. Chem. Soc.*, 1971, **93**, 4126–4136.

88. A. A. Frimer, *Singlet Oxygen, Volume 2: Reaction Modes and Products, Part I*, CRC Press, Boca Raton, 1985.

89. W. Adam, C. R. Saha-Möller, and S. B. Schambony, *J. Am. Chem. Soc.*, 1999, **121**, 1834–1838.

90. W. Adam, S. G. Bosio, and N. J. Turro, *J. Am. Chem. Soc.*, 2002, **124**, 8814–8815.

91. T. Poon, J. Sivaguru, R. Franz, *et al*., *J. Am. Chem. Soc.*, 2004, **126**, 10498–10499.

92. M. A. Avery, C. Jennings-White, and W. K. M. Chong, *J. Org. Chem.*, 1989, **54**, 1789–1792.

93. P. A. Burns and C. S. Foote, *J. Am. Chem. Soc.*, 1974, **96**, 4339–4340.

94. R. N. Bagchi, A. M. Bond, F. Scholz, and R. Stösser, *J. Am. Chem. Soc.*, 1989, **111**, 8270–8271.

95. K. Ohkubo, S. C. Menon, A. Orita, *et al*., *J. Org. Chem.*, 2003, **68**, 4720–4726.

96. S. F. Nelsen and R. Akaba, *J. Am. Chem. Soc.*, 1981, **103**, 2096–2097.

97. S. F. Nelsen, D. L. Kapp, R. Akaba, and D. H. Evans, *J. Am. Chem. Soc.*, 1986, **108**, 6863–6871.

98. E. L. Clennan, W. Simmons, and C. W. Almgren, *J. Am. Chem. Soc.*, 1981, **103**, 2098–2099.

99. S. F. Nelsen, D. L. Kapp, F. Gerson, and J. Lopez, *J. Am. Chem. Soc.*, 1986, **108**, 1027–1032.

100. M. Kamata, J. Kaneko, J. Hagiwara, and R. Akaba, *Tetrahedron Lett.*, 2004, **45**, 7423–7428.

101. K. Ohkubo, T. Nanjo, and S. Fukuzumi, *Catal. Today*, 2006, **117**, 356–361.

102. F. D. Lewis, J. R. Petisce, J. D. Oxman, and M. J. Nepras, *J. Am. Chem. Soc.*, 1985, **107**, 203–207.

103. J. Eriksen and C. S. Foote, *J. Am. Chem. Soc.*, 1980, **102**, 6083–6088.

104. L. E. Manring, J. Eriksen, and C. S. Foote, *J. Am. Chem. Soc.*, 1980, **102**, 4275–4277.

105. L. T. Spada and C. S. Foote, *J. Am. Chem. Soc.*, 1980, **102**, 391–393.

106. T. Yamashita, T. Tsurusako, N. Nakamura, *et al*., *Bull. Chem. Soc. Jpn.*, 1993, **66**, 857–862.

107. T. Inoue, K. Koyama, T. Matsuoka, and S. Tsutsumi, *Bull. Chem. Soc. Jpn.*, 1967, **40**, 162–168.

108. S. Futamura, H. Ohta, and Y. Kamiya, *Chem. Lett.*, 1982, 381–384.

109. M. Tsuchiya, T. W. Ebbesen, Y. Nishimura, *et al*., *Chem. Lett.*, 1987, 2121–2124.

110. S. Konuma, S. Aihara, Y. Kuriyama, *et al*., *Chem. Lett.*, 1991, 1897–1900.

111. S. Tojo, K. Morishima, A. Ishida, *et al*., *J. Org. Chem.*, 1995, **60**, 4684–4685.

112. T. Majima, S. Tojo, A. Ishida, and S. Takamuku, *J. Phys. Chem.*, 1996, **100**, 13615–13623.

113. F. D. Lewis, R. E. Dykstra, I. R. Gould, and S. Farid, *J. Phys. Chem.*, 1988, **92**, 7042–7043.

114. Y. Kuriyama, T. Arai, H. Sakuragi, and K. Tokumaru, *Chem. Phys. Lett.*, 1990, **173**, 253–256.

115. T. Majima, S. Tojo, A. Ishida, and S. Takamuku, *J. Org. Chem.*, 1996, **61**, 7793–7800.

116. F. D. Lewis, A. M, Bedell, R. E. Dykstra, *et al*., *J. Am. Chem. Soc.*, 1990, **112**, 8055–8064.

117. G. Franz and R. A. Sheldon, *Ullmann's Encyclopedia of Industrial Chemistry*, 5th edn, VCH, Weinheim, Germany, 1991.

118. R. A.; Sheldon and J. K. Kochi, *Metal Catalyzed Oxidation of Organic Compounds*, Academic Press, New York, 1981, chap. 10.

119. R. E. Ballard and A. McKillop, U.S. Patent 4,482,438, 1984.

120. R. Clarke, A. Kuhn, and E. Okoh, *Chem. Br.*, 1975, **11**, 59–64.

121. L. Syper, *Tetrahedron Lett.*, 1966, 4493–4498.

122. T.-L. Ho, *Synthesis*, 1973, 347–354.

123. M. Oelgemöller, C. Jung, J. Ortner, *et al*., *Green Chem.*, 2005, **7**, 35–38.

124. F. Cavani and J. H. Teles, *ChemSusChem*, 2009, **2**, 508–534.

125. W. T. Hess, *Kirk-Othmer Encyclopedia of Chemical Technology*, 4th edn, Wiley, New York, 1995, vol. 13, p. 961.

126. A. Das, V. Joshi, D. Kotkar, *et al.*, *J. Phys. Chem. A*, 2001, **105**, 6945–6954.

127. W. Song, J. Ma, C. Chen, and J. Zhao, *J. Photochem. Photobiol. A: Chem.*, 2006, **183**, 31–34.

128. M. A. Fox, *Photoinduced Electron Transfer*, ed. M. A. Fox and M. Chanon, Elsevier, Amsterdam, 1988, pp. 1–27.

129. M. Julliard, C. Legris, and M. Chanon, *J. Photochem. Photobiol. A: Chem.*, 1991, **61**, 137–152.

130. K. Ohkubo and S. Fukuzumi, *Bull. Chem. Soc. Jpn.*, 2009, **82**, 303–315.

131. K. Ohkubo, K. Suga, K. Morikawa, and S. Fukuzumi, *J. Am. Chem. Soc.*, 2003, **125**, 12850–12859.

132. K. Suga, K. Ohkubo, and S. Fukuzumi, *J. Phys. Chem. A*, 2005, **109**, 10168–10175.

133. M. Fujita, A. Ishida, S. Takamuku, and S. Fukuzumi, *J. Am. Chem. Soc.*, 1996, **118**, 8556–8574.

134. K. Ohkubo, K. Mizushima, R. Iwata, *et al.*, *Chem. Commun.*, 2010, **46**, 601–603.

135. A. G. Griesbeck and M. Cho, *Org. Lett.*, 2007, **9**, 611–613.

136. J. Santamaria, P. Gabillet, and L. Bokobza, *Tetrahedron Lett.*, 1984, **25**, 2139–2142.

137. K. Ohkubo, T. Nanjo, and S. Fukuzumi, *Bull. Chem. Soc. Jpn.*, 2006, **79**, 1489–1500.

138. M. Nakamura, M. Miki, and T. Majima, *J. Chem. Soc. Perkin Trans. 2*, 2000, 1447–1452.

139. S. Tsuji, M. Kondo, K. Ishiguro, and Y. Sawaki, *J. Org. Chem.*, 1993, **58**, 5055–5059.

140. D. G. Ho, R. Gao, J. Celaje, *et al.*, *Science*, 2003, **302**, 259–262.

141. F. D. Lewis and T.-I. Ho, *J. Am. Chem. Soc.*, 1977, **99**, 7991–7996.

142. S. Naya, H. Ohtoshi, and M. Nitta, *J. Org. Chem.*, 2006, **71**, 176–184.

143. S. Naya, J. Nishimura, and M. Nitta, *J. Org. Chem.*, 2005, **70**, 9780–9788.

144. B. Armitage, *Chem. Rev.*, 1998, **98**, 1171–1200.

145. I. E. Kochevar and D. A. Dunn, *Bioorg. Photochem.*, 1990, **1**, 273–315.

146. M. E. Núñez, S. R. Rajski, and J. K. Barton, *Methods Enzymol.*, 2000, **319**, 165–188.

147. J. Kim, M. F. Sistare, P. J. Carter, and H. H. Thorp, *Coord. Chem. Rev.*, 1998, **171**, 341–350.

148. T. Da Ros, G. Spalluto, A. S. Boutorine, *et al.*, *Curr. Pharm. Design*, 2001, **7**, 1781–1821.

149. R. Bonnett, *Metal Complexes for Photodynamic Therapy, Comprehensive Coordination Chemistry II*, eds. J. A. McCleverty and T. J. Meyer, Elsevier, Oxford, 2004, vol. 9, pp. 945–1003.

150. K. Ohkubo, K. Yukimoto, and S. Fukuzumi, *Chem. Commun.*, 2006, 2504–2506.

151. M. Tanaka, K. Yukimoto, K. Ohkubo, and S. Fukuzumi, *J. Photochem. Photobiol. A: Chem.*, 2008, **197**, 206–212.

152. S. Fukuzumi, H. Miyao, K. Ohkubo, and T. Suenobu, *J. Phys. Chem. A*, 2005, **109**, 3285–3294.

153. K. Kobayashi and S. Tagawa, *J. Am. Chem. Soc.*, 2003, **125**, 10213–10218.

154. L. P. Candeias and S. Steenken, *J. Am. Chem. Soc.*, 1989, **111**, 1094–1099.

155. J.-P. Lecomte, A. Kirsch-De Mesmaeker, M. M. Feeney, and J. M. Kelley, *Inorg. Chem.*, 1995, **34**, 6481–6491.

156. I. Ortmans, B. Elias, J. M. Kelly, *et al.*, *Dalton Trans.*, 2004, 668–673.

157. C. J. Burrows and J. G. Muller, *Chem. Rev.*, 1998, **98**, 1109–1152.

158. C. Bohne, K. Faulhaber, B. Giese, *et al.*, *J. Am. Chem. Soc.*, 2005, **127**, 76–85.

159. K. Ohkubo, K. Mizushima, R. Iwata, and S. Fukuzumi, *Chem. Sci.*, 2011, **2**, 715–722.

160. G. K. S. Prakash, T. Mathew, D. Hoole, *et al.*, *J. Am. Chem. Soc.*, 2004, **126**, 15770–15776.

161. F. Kakiuchi, T. Kochi, H. Mutsutani, *et al.*, *J. Am. Chem. Soc.*, 2009, **131**, 11310–11311.

162. E. Baciocchi, C. Crescenzi, and O. Lanzalunga, *Tetrahedron*, 1997, **53**, 4469–4478.

163. J. Eriksen, C. S. Foote, and T. L. Parker, *J. Am. Chem. Soc.*, 1977, **99**, 6455–6456.

164. N. Soggiu, H. Cardy, J. L. Habib, and J. P. Soumillon, *J. Photochem. Photobiol. A*, 1999, **124**, 1–8.

165. E. Baciocchi, T. Del Giacco, F. Elisei, *et al.*, *J. Am. Chem. Soc.*, 2003, **125**, 16444–16454.

166. Y. Che, W. Ma, Y. Ren, *et al.*, *J. Phys. Chem. B*, 2005, **109**, 8270–8276.

167. S. Lacombe, H. Cardy, M. Simon, *et al.*, *Photochem. Photobiol. Sci.*, 2002, **1**, 347–354.

168. T. Pigot, T. Arbitre, M. Hervé, and T. S. Lacombe, *Tetrahedron Lett.*, 2004, **45**, 4047–4050.

169. V. Latour, T. Pigot, M. Simon, *et al.*, *Photochem. Photobiol. Sci.*, 2005, **4**, 221–229.

170. S. M. Bonesi, I. Manet, M. Freccero, *et al.*, *Chem. Eur. J.*, 2006, **12**, 4844–4857.

171. K. T. Potts, M. J. Cipullo, P. Ralli, and G. Theodoridis, *J. Org. Chem.*, 1982, **47**, 3027–3038.

172. P. Arsenyan, E. Paegle, and S. Belyakov, *Tetrahedron Lett.*, 2010, **51**, 205–208.

173. P. Arsenyan, O. Pudova, J. Popelis, and E. Lukevics, *Tetrahedron Lett.*, 2004, **45**, 3109–3111.

174. T. J. Dingemans, N. S. Murthy, and E. T. Samulski, *J. Phys. Chem. B*, 2001, **105**, 8845–8860.

175. M. M. Murray, P. Kaszynski, D. A. Kaisaki, *et al.*, *J. Am. Chem. Soc.*, 1994, **116**, 8152–8161.

176. D. T. Sawyer, T. S. Calderwood, K. Yamaguchi, and C. T. Angelis, *Inorg. Chem.*, 1983, **22**, 2577–2583.

177. A. Podgorsek, S. Stavber, M. Zupan, and J. Iskra, *Tetrahedron*, 2009, **65**, 4429–4439.

178. K. Ohkubo, R. Iwata, T. Yanagimoto, and S. Fukuzumi, *Chem. Commun.*, 2007, 3139–3142.

179. S. Fukuzumi, H. Mori, H. Imahori, *et al.*, *J. Am. Chem. Soc.*, 2001, **123**, 12458–12465.

180. C. A. Reed and R. D. Bolskar, *Chem. Rev.*, 2000, **100**, 1075–1120.

181. S. Fukuzumi, H. Mori, T. Suenobu, *et al.*, *J. Phys. Chem. A*, 2000, **104**, 10688–10694.

182. D. Dubois, G. Moninot, W. Kutner, *et al.*, *J. Phys. Chem.*, 1992, **96**, 7137–7145.

183. M. Fujitsuka, C. Luo, O. Ito, *et al.*, *J. Phys. Chem. A*, 1999, **103**, 7155–7160.

184. K. Ohkubo, R. Iwata, S. Miyazaki, *et al.*, *Org. Lett.*, 2006, **8**, 6079–6082.

185. H. Bouas-Laurent, A. Castellan, J.-P. Desvergne, and R. Lapouyade, *Chem. Soc. Rev.*, 2000, **29**, 43–55.

186. H. Bouas-Laurent, A. Castellan, J.-P. Desvergne, and R. Lapouyade, *Chem. Soc. Rev.*, 2001, **30**, 248–263.
187. J. L. Charlton, R. Dabestani, and J. Saltiel, *J. Am. Chem. Soc.*, 1983, **105**, 3473–3476.
188. H.-D. Becker, K. Andersson, and K. Sandros, *J. Org. Chem.*, 1980, **45**, 4549–4555.
189. H.-D. Becker, S. R. Hall, B. W. Skelton, and A. H. White, *Aust. J. Chem.*, 1984, **37**, 1313–1327.
190. M.-J. Fernández, L. Gude, and A. Lorente, *Tetrahedron Lett.*, 2001, **42**, 891–893.
191. G. Felix, R. Lapouyade, A. Castellan, *et al*., *Tetrahedron Lett.*, 1975, **16**, 409–412.
192. L. A. Deardurff, M. S. Alnajjar, and D. M. Camaioni, *J. Org. Chem.*, 1986, **51**, 3686–3693.
193. M. Horiguchi and Y. Ito, *J. Org. Chem.*, 2006, **71**, 3608–3611.
194. W. Adam, K. Schneider, M. Stapper, and S. Steenken, *J. Am. Chem. Soc.*, 1997, **119**, 3280–3287.
195. H. Higuchi, T. Otsubo, F. Ogura, *et al*., *Bull. Chem. Soc. Jpn.*, 1982, **55**, 182–187.

Please note that the abstract and keywords will not be included in the printed book, but are required for the online presentation of this book which will be published on Wiley's own online publishing platform.

If the abstract and keywords are not present below, please take this opportunity to add them now. The abstract should be a short paragraph upto 200 words in length and keywords between 5 and 10 words.

Abstract: This article describes the recent development of photocatalytic reactions using a simple donor-acceptor-linked dyad, 9-mesityl-10-methylacridinium ion (Acr$^+$–Mes). The electron-transfer state of Acr$^+$–Mes (Acr$^{\bullet}$–Mes$^{\bullet+}$), produced on visible light irradiation, acts as an efficient oxidant and reductant. The use of Acr$^+$–Mes, which has an extremely long-lived charge-separated state, enables the construction of highly efficient photocatalytic systems such as oxygenation, bromination, and carbon-carbon bond formation of aromatic compounds.